Chemical Geology 514 (2019) 122–137

Contents lists available at ScienceDirect

Chemical Geology

journal homepage: www.elsevier.com/locate/chemgeo

Invited research article

Biogeochemical mechanisms controlling phosphorus diagenesis and internal loading in a remediated hard water eutrophic embayment

Stefan Markovic[a], Anqi Liang[a], Sue B. Watson[c], Jay Guo[c], Shan Mugalingam[d], George Arhonditsis[b], Andrew Morley[e], Maria Dittrich[a,*]

[a] Biogeochemistry Group, Department of Physical and Environmental Sciences, University of Toronto Scarborough, 1265 Military Trail, Toronto M1C1A4, Ontario, Canada
[b] Ecological Modeling Group, Department of Physical and Environmental Sciences, University of Toronto Scarborough, 1265 Military Trail, Toronto M1C 1A4, Ontario, Canada
[c] Department of Biology University of Waterloo, Waterloo N2L 3G1, Ontario, Canada
[d] Lower Trent Region Conservation Authority, 714 Murray Street, Trenton K8V 5P4, Ontario, Canada
[e] Kingston Regional Office, Ontario Ministry of the Environment and Climate Change, Kingston K7M 8S5, Ontario, Canada

ARTICLE INFO

Editor: Karen Johannesson

Keywords:
Lake sediment
Phosphorus
Early diagenesis
Internal loading
Phosphorus binding forms
Shallow eutrophic embayment
Lake Ontario

ABSTRACT

Phosphorus (P) levels in eutrophic lakes with restricted external P inputs often show hysteresis resulting from sediment P diagenetic recycling. Hard water oxygenated lakes are often thought to be less susceptible to P release from sediment due to precipitation of P with calcium carbonate and P sorption on iron (Fe) oxyhydroxides in oxidized surface sediments. However, perpetuated eutrophic conditions in many hard water oxygenated lakes persist despite drastic reduction of external P inputs. What limits P sediment binding capacity and drives its release from sediments in such lakes is often less understood. Here we characterize sediment P diagenetic processes driving persistent internal loading in the Bay of Quinte, a hard water, polymictic embayment of Lake Ontario, Canada. We used a multifaceted approach, combining a comprehensive three-year study of sediment P binding forms, recent sediment stratigraphy and accumulation, high spatial resolution measurement of dissolved oxygen, redox potential and pH across the sediment-water interface and depth profiles of nutrient and metals concentrations in pore water. Despite oxygenated bottom water conditions P diffusive fluxes during summer are substantial (1–6.5 mg P/m^2/day), representing as much as 50% of external P inputs. Estimated rates of benthic organic carbon degradation indicate that anaerobic organic P mineralization in anoxic sediments is the main driver of P release, which is strongly influenced by Fe reduction. Estimated rates of benthic organic carbon degradation indicate that anaerobic organic P mineralization in anoxic sediments is the main driver of P release. In surface sediment the redox sensitive P is the prevailing diagenetically reactive P phase, emphasizing strong coupling with ferric Fe. While this indicates substantial P sorption on Fe oxyhydroxides, their spare binding capacity is limited, as reducible Fe: P ratios are close to sorption limit. The calcium carbonate bound P increased with sediment depth at the expense of redox sensitive P, suggesting diagenetic sequestration into apatite with sediment burial. However, only 40% of diagenetically reactive P forms, which account for ~2/3 of the total P in surface sediment, are permanently retained during burial. Importantly, our data show that in fact significant P-flux occurs in shallow areas, with an apparent discordance with concurrent measures of long-term P release from the sediments. These results also demonstrate that short-term measures cannot be extrapolated to long-term estimates and vice versa.

1. Introduction

While phosphorus (P) is an essential macronutrient for maintaining primary production in freshwater ecosystems, excessive concentrations lead to undesirable algal blooms, anoxic bottom water and loss of biodiversity (e.g., Smith and Schindler, 2009). Lakes are prone to accumulating P from various sources, including riverine inputs, agricultural runoff, sewage and industrial effluents. Under favorable biogeochemical conditions, the legacy P accumulated in sediments can be released to the overlaying water column for many decades, effectively delaying management efforts to reduce external P inputs (Katsev and Dittrich, 2013). Despite its crucial role in the recovery of ecosystems,

* Corresponding author.
E-mail address: mdittrich@utsc.utoronto.ca (M. Dittrich).

https://doi.org/10.1016/j.chemgeo.2019.03.031
Received 11 May 2018; Received in revised form 23 March 2019; Accepted 27 March 2019
Available online 31 March 2019
0009-2541/

sediment P diagenesis and release in many lakes undergoing extensive changes, such as urbanization, reduction of external loading, remain poorly understood (Orihel et al., 2017).

Shallow nearshore environments and wetlands have recently received a lot of attention and increasingly became focus of sediment P biogeochemical studies (Parsons et al., 2017). These habitats are highly sensitive to anthropogenic influences (e.g., warming climate, habitat destruction and changing external P inputs (Orihel et al., 2017)). Diagenetic P recycling in these environments is complex, dynamic process and exhibits a strong spatial and temporal heterogeneity (Depew et al., 2018; Matisoff and Lou Carson, 2014; Matisoff et al., 2016; Parsons et al., 2017; Ozersky et al., 2013). Yet there remains considerable controversy surrounding P diagenesis. For example, sediment P release in shallow water bodies is thought to be suppressed by P sorption on iron oxyhydroxides. However, sediment P recycling is shown to be partly limited by its vertical redistribution between P binding forms during sediment diagenesis (Parsons et al., 2017). The influence of P transformations from labile binding forms to Ca-carbonates and Ca-phosphates in hard water environments is particularly important, as these phases are stable and redox insensitive thus representing permanent P sink which has not been systematically studied in shallow aquatic systems (Dittrich and Koschel, 2002).

Diagenetic processes return mobile (diagenetically reactive) P forms from the sediments to the water column and sequester a portion of P into refractory forms, which are permanently buried. The potentially mobile forms include loosely sorbed P, P adsorbed to redox-sensitive metallic oxides (e.g., Fe-oxy-hydrooxides) and reactive organic P (polyphosphates, phospholipids and DNA/RNA) (Rydin, 2000; Paraskova et al., 2014). The refractory or immobile pool, which is stable over long time periods under typical pH and redox conditions, includes refractory organic matter, apatite and P sorbed on Al hydroxides under stable neutral to low pH (Kopáček et al., 2005). Although originating in operational techniques, sequential P extraction helps determine the abundance of different binding forms, track and compare their transformation during diagenesis. Changes in the concentration of different P binding forms with sediment depth are used to estimate the long-term rate of diagenetic P transformations and recycling and to quantify the size and composition of potentially mobile P pool temporarily stored in sediments (e.g., Rydin et al., 2011; Hupfer and Lewandowski, 2005; Dittrich et al., 2013).

Despite the importance of diagenetic processes, sediment P binding forms and processes controlling their transformation (e.g., P transfers from potentially mobile to more stable binding forms) are unresolved in many eutrophic water bodies and usually not considered in remedial plans. This is significant omission because P diagenetic transfers from labile to inert P forms are the principal mechanisms of long-term P retention and define sediment response to loading reduction. Even though P binding forms are quantified in some lakes using common sequential extraction schemes, the metals associated with extracted P pools are not routinely measured. Yet, ratios of metals and P (e.g, Fe:P or Al:P ratios) in extraction pools are indicative of the underlying processes controlling P release and retention, and these ratios can inform eutrophication management decisions (e.g., Kopáček et al., 2005; Geurts et al., 2008).

Moreover, sediment P recycling is traditionally assessed as representing the short-term (days/weeks/months) biogeochemical redox processes of iron oxyhydroxide dissolution resulting from hypolimnetic and sediment anoxia, which affects diurnal and seasonal P levels in the water column (Hupfer and Lewandowski, 2008). Redox processes are crucial to estimate P diffusive fluxes over a short time-scale (e.g., Tammeorg et al., 2015). However, diagenetic P mobilization and immobilization are transient and reversible processes. In shallow eutrophic systems, the majority of P released during reductive dissolution of iron oxyhydroxides is redistributed between different solid P binding pools (e.g., Parsons et al., 2017). The reallocation of P between different mineral and organic binding pools needs to be considered, in order to understand the P release on long-term scales (years to decades), which primarily stems from an imbalance between sedimentation supply of labile P forms and sediment capacity to bind P in inert phases (Katsev et al., 2006; Hupfer and Lewandowski, 2008; Katsev and Dittrich, 2013).

Katsev et al. (2006) showed that short- and long-term P release and retention need to be considered separately because processes controlling P release on daily and seasonal time scales are different from processes controlling P burial and recycling on long-term time scales. For instance, while P released from freshly deposited organic matter may be temporarily prevented from re-entering overlaying water column by P sorption on Fe oxyhydroxides in surface sediment as classical Mortimer (1942) study suggests, this does not necessarily control P release on the long-term time scales because eventual burial of P enriched layers in anoxic sediment may result in complete dissolution of Fe oxyhydroxides and release of P (Katsev et al., 2006). On the other hand, desorption of P from Fe oxyhydroxides may increase pore water P concentration and consequently, saturation state in respect to stable P phases such as vivianite or Ca-phosphates thereby promoting permanent P sequestration (Katsev et al., 2006). Especially in case of shallow oxygenated lakes, where costly and extensive efforts to reduce of external P loading have yielded only modest improvements of water quality, a role of sediment in P cycling on both short- and long-term has been underestimated. This is important oversight because nutrient reduction strategies in any watershed necessitate comprehensive understanding of the amount and long-term mobility of the diagenetically reactive sediment P to better assess external load reduction needs.

The Bay of Quinte is representative of many shallow eutrophic systems across the world, with a long history of eutrophication and associated legacy of highly organic, nutrient rich sediments. Presently the Bay is showing a delayed recovery following an extended period of intensive external P loading reduction (Minns et al., 1986; Minns et al., 2011; Kim et al., 2013). This water body develops annual blooms of potentially toxic cyanobacteria (Shimoda et al., 2016). Despite a rapid flushing rate (4–5 times/year, Shore et al., 2016) and drastically reduced P inputs (> 90%) for over three decades, Minns et al., 2011), summer surface water TP concentrations are persistently elevated (45–50 TP μg/l, Shimoda et al., 2016). The failure of the intensive restoration efforts reflected in a persistent harmful algal blooming initiated a suite of modelling studies, which aimed to understand P balance in this system (Kim et al., 2013; Arhonditsis et al., 2016). The modelling studies proposed that sediment might provide a hitherto underestimated internal P source. This conclusion based on mass balance modelling, is surprising from a geochemical perspective. Firstly, as a hard water lake system, the Bay of Quinte would be expected to be less prone to internal P loading due to presence of permanent P sinks in the form of Ca-carbonates and Ca-phosphates in hard-water environments (Dittrich and Koschel, 2002). Secondly, oxygenated bottom waters are associated with presence of iron oxyhydroxide barrier in surface sediments suppressing diffusive P fluxes (Katsev et al., 2006; Hupfer and Lewandowski, 2008; Katsev and Dittrich, 2013). Thirdly, short hydraulic residence time would suggest prompt response to external loading reduction (Katsev, 2017). Despite international prominence of this area as the officially listed Area of Concern (AOC) under the bilateral agreement on the Great Lakes water quality between the United States and Canada, sediment P diagenesis has not been investigated and consequently, the mechanisms of diagenetic recycling and sequestration are not understood. The details of the sediment P release have so far been deduced from water column P concentration measurements and whole lake nutrient budget models. Consequently, the chemical speciation of sedimentary P, the size and composition of diagenetically mobile P pool and its transformation and mobilization pathways remain unknown.

Against this background, our study was setup to test the hypothesis that diagenetic P recycling in shallow hardwater lakes may persist for

several decades, despite oxygenated water with short renewal time, as well as steep and prolonged reduction of external P inputs. We tested the premise that reducing conditions mobilize labile P forms (Fe bound P and organic P) temporarily stored in diagenetically active and organic rich shallow sediment. Furthermore, we hypothesized that diagenetic transformation of labile P forms during burial leads to authigenesis of inert Ca-P phases which drives the long-term sediment P retention.

We used a multifaceted approach, combining a comprehensive multiyear study of sediment P binding forms, recent sediment stratigraphy and accumulation, measurements of dissolved oxygen uptake, redox potential and pH across the sediment-water interface and depth profiles of nutrient and metals concentrations in pore water. Our study had the following objectives: 1) Estimate and compare short-term diffusive P fluxes during consecutive summer seasons in three limnologically different basins of the large and shallow embayment. 2) Quantify long-term P diagenetic release and retention and the size of temporarily stored P binding pools. 3) Clarify the factors controlling P diagenesis and delineate the underlying mechanisms behind long-term sediment P release and retention, which involves P sorption/desorption, authigenesis, organic matter mineralization and cumulative diagenetic redistribution between labile and inert P forms. Our findings emphasized that diagenetically reactive sediment P pool needs to be explicitly considered in any lake nutrient management strategy even after decades of successful external nutrient control measures and we believe that example presented here will be of relevance to many similar systems worldwide.

2. Methods

2.1. Site description

The Bay of Quinte is a eutrophic, *Z*-shaped embayment on the northern shore of Lake Ontario. The bay is narrow, with a total length of 64 km, a maximum width of 3.5 km and a surface area of 254 km^2 (Fig. 1). Glacial scouring of pre-glacial river valleys sculptured a series of connected basins that gradually increased in depth from ~2 m mid-channel near Trenton to ~60 m near Amherst Island, where the bay meets the Kingston basin of Lake Ontario (Sly, 1986).

The watershed of the Bay of Quinte is ~70 times its surface area and covers ~18,000 km^2. The major tributaries are the Trent River, Wilton Creek, and the Moira, Salmon and Napanee rivers, all of which enter the upper and middle section of the bay along the northern shore. The geology of the watershed consists of igneous and metasedimentary rocks of the Precambrian Canadian Shield in the north (Trent, Moira and Napanee rivers headwater region) and extensive Paleozoic clayey limestone bedrock with thin overburden formed by glacial till and glacio-lacustrine sand and clay deposits (Sly, 1986; Armstrong and Dodge, 2007). Due to prevalence of carbonate bedrock, the Bay of Quinte water is well buffered with the alkalinity of the lake water ~100 mg $CaCO_3$ equivalent and typical pH ranges between 8.0 and 8.5 (see compilation dataset from Currie and Frank, 2015).

Extensive forest clearance and intensive agriculture, compounded by population growth in the Bay of Quinte watershed since the mid-19th century, resulted in progressive eutrophication of the upper bay, which was eutrophic as early as the 1920s (Warwick, 1980; Stoermer et al., 1985). Cultural eutrophication processes are particularly severe in the upper and middle Bay of Quinte, where most of the population lives and where all major tributaries discharge.

In this study, three sampling sites located in the upper and middle bay were chosen based on trophic status and beneficial use impairment. The Belleville site (station B, 44°9′15″ N, 77°20′45.00″ E; maximal water depth (Z_{max}) 4.6 m) is located offshore from the city of Belleville, ~2 km from the mouth of the Moira River, and along with the Hay Bay site, it is one of the federal long-term monitoring sites. It is assumed to represent the conditions in the upper bay (Currie and Frank, 2015). The Napanee site (station N, 44°10′49.00″ N, 77°2′25″ E; maximal water depth 5 m) is located offshore from the town of Deseronto, proximal to the mouth of the Napanee River. Station N represents a transitional zone between the upper bay and the middle bay. The Hay Bay site (station HB, 44°6′25.00″ N, 77°1′51″ E; water depth 15 m) is the middle bay site located south of Ram Island in Hay Bay.

2.2. Sediment sampling

Samples were collected from the three stations, B, N and HB, using a gravity corer (UWITEC, Austria) and polycarbonate core liners 5.5 cm in diameter and ca. 70 cm in length. Sampling times are shown in Table S1. Six to seven cores per station were collected during each sampling. The sediment cores were sealed and transported to the laboratory in a thermo-isolated box for storage at ~4 °C.

In the laboratory, the cores were first logged prior to sectioning to differentiate the sedimentary layers, then sectioned for the analysis of P binding forms, metal contents in P fractions, porosity, dry weight, total organic matter and dissolved substances.

Fig. 1. Sampling location for three stations in the Bay of Quinte.

2.3. Chronology and sedimentation rates

One sediment core per site was sliced into 1 cm intervals for dating, by Flett Research Laboratory (Winnipeg, Canada), using the ^{210}Pb method. Lead-210 was measured as ^{210}Po by alpha spectrometry in sample residue after digestion in nitric acid. Prior to digestion, samples were first spiked with a Po-209 to monitor the yield. The background ^{210}Pb activity was determined from ^{226}Ra activity by ^{220}Rn emanation analysis using the method by Mathieu et al. (1988). The depth profiles of excess ^{210}Pb activity were calculated by subtracting background ^{210}Pb from the total ^{210}Pb activity (expressed hereafter in disintegrations per minute per g, or DPM/g). The sediment age-depth relationship and mass accumulation rates were calculated using this accumulated excess ^{210}Pb activity and measured dry bulk density (dry weight per volume of wet sediment), assuming the constant rate of supply (CRS) model (Appleby and Oldfield, 1978).

2.4. Depth profiles of dissolved O_2, H_2S, pH and redox potential

Dissolved oxygen (DO), H_2S, pH and redox measurements were carried out ex situ onshore, immediately after sampling using microelectrodes, on at least one core per site. Vertical profiles of O_2, H_2S, pH and redox were measured simultaneously from the overlying water into the sediment, by lowering microelectrodes mounted on a stand fitted with a Vernier caliper.

Each oxygen, sulfide, pH, and redox profile presented hereafter represents the average of replicate measurements from the same sediment core. The standard deviation of repeated oxygen and pH measurements was < 5%, while it was < 10% for H_2S and redox measurements.

2.5. Phosphorus binding forms

We extracted sediment P binding forms using P fractionation technique adapted from Psenner and Pucsko (1988), with modifications by Hupfer et al. (2009). This technique separates sediment P into the following fractions: (a) loosely adsorbed (labile) P (extracted with NH_4Cl, NH_4Cl-P); (b) redox-sensitive P bound to Fe and Mn oxyhydroxides (extracted with bicarbonate dithionite (BD), BD-P); (c) P bound to hydrated oxides of aluminum, clays (extracted with NaOH, NaOH-SRP); (d) organic bound P (extracted with NaOH, NAOH-NRP); and (e) calcium-bound P (HCl-P) (extracted with HCl) f) refractory P (Ref-P) (Hupfer et al., 1995; Hupfer et al., 2009). These sediment P fractions are operationally defined, i.e., each fraction is defined by an extraction solution representing specific pH and redox conditions and therefore incorporates a diverse pool of P chemical species, e.g., NaOH-SRP represents a pool of P species exchangeable with hydroxyl ion, which includes P sorbed on Al hydroxides, clays and non-reducible inorganic P compounds soluble at elevated pH (Fe and Al hydroxyl-phosphates) (Lukkari et al., 2007; Hupfer et al., 2009). During each extraction step, metal ions associated with specific P phases are mobilized in addition to targeted P species. These metal(-oid) pools associated with P fractions provide additional insight into P composition and its diagenetic transformation (e.g., Lukkari et al., 2007; Norton et al., 2008). Thus, in this study, we analyzed the content of Fe, Al, Ca, Mn, Si in each P fraction.

2.6. Porosity and total organic carbon and organic nitrogen

Sediment water content was measured by drying at 105 °C for 60 h. Loss on ignition (LOI) was calculated as the loss of weight during ignition at 550 °C for 4 h. The total carbon has been estimated as $OC = LOI_{550}/2.5$ (i.e., assuming organic matter composition as CH_2O, Burdige, 2006). Dry weight (water content), porosity (calculated using moisture loss during drying), and loss on ignition represent the average of two samples from the same layer.

In addition to organic matter estimation using loss on ignition, organic C and N in freeze-dried surface sediments from August 2014 and October 2014 were analyzed by CN628 elemental analyzer (LECO Instruments ULC, Canada).

2.7. Pore water sampling

Pore water was extracted using passive in situ samplers, or peepers. Each custom-made peeper consisted of a Plexiglas base plate body with sampling wells and one face plate of high-density polyethylene (HPDE) held together with stainless-steel screws and washers. The distance between sampling wells was 1 cm. STERLITECH Polyethersulfone dialysis membrane (pore size: 0.20 μm) was placed between the base plate and the face plate. Peeper chambers (sampling wells) were filled with deionized water and purged with N_2. The peepers were kept in oxygen-free (N_2 purged) Plexiglas chambers prior to deployment in the field. At each station, duplicate peepers were used.

The equilibration time was 1 to 2 weeks (see Table S1). Upon retrieval, pore water was immediately syringed and divided into separate vials for analysis of dissolved cations, NH_4^+, SO_4^{2-} and soluble reactive phosphorus (SRP). Samples were preserved following standard guidelines U.S. EPA (1982).

2.8. Chemical analyses of P fractions and pore water

The concentrations of major elements (P, Fe, Al, Ca, Mn, Si) in P extraction pools and of P in pore water samples collected during 2013–2015 were measured by Inductive Coupled Plasma Mass Spectrometry (ICP-MS) at Water Quality Center, Trent University.

Metals (Fe, Al, Ca, Mn, Si) and SRP from samples collected during May and August 2015 sampling were analyzed using ICP-MS at Trent University. Pore water samples collected on other dates during 2014 and 2015 were analyzed at the University of Toronto: SRP was analyzed using Ascorbic Acid-Molybate spectrophotometric assay, while cations (Fe, Al, Ca, Mn, Si) were analyzed using Agilent Inductive Coupled Plasma Atomic Emission Spectroscopy (ICP-AES).

SRP, Fe (II) and NH_4^+ in pore water samples collected during 2016 were analyzed at the University of Toronto using the micro-spectrophotometric methods described in detail in Laskov et al. (2007).

Samples were run in triplicate and the relative standard deviation for different measured variables was under 10%. The data quality assurance and control was ensured through the use of standard procedures, including method blanks, and spiked and blind reference samples. Standard reference samples were used to cross-calibrate measurements using different methods.

2.9. Potentially mobile P

The depth profile of sediment P commonly shows downward decrease, with maximum P concentrations in the surface layers and constant concentrations in deeper layers (see compilation of sediment P profiles of different lakes, Carey and Rydin, 2011). The depth at which there is no changes in P concentration with depth (gradient equals 0) represents the stabilization depth of P, beyond which the remaining P is assumed to be permanently buried (see illustration in Fig. S1). The stabilization of diagenetic processes depends on a number of factors, including sediment accumulation (burial) rate, dynamics of external inputs, and internal P recycling and physical processes (resuspension, bioturbation, sediment focusing) (Søndergaard et al., 2003). Solid P in surface sediment exceeding P concentration at stabilization depth can be assumed to be mobile and to represent the temporary sediment storage expressed as the mass of P per m^2 (e.g., Rydin, 2000; Carey and Rydin, 2011; Rydin et al., 2011; Malmaeus et al., 2012; Puttonen et al., 2014; Hupfer and Lewandowski, 2005). This potentially mobile P was calculated following the method described in Rydin et al. (2011):

$$P_{mobile} = \sum_{i=1}^{n} \Delta C_i \rho_i x_i \quad (1)$$

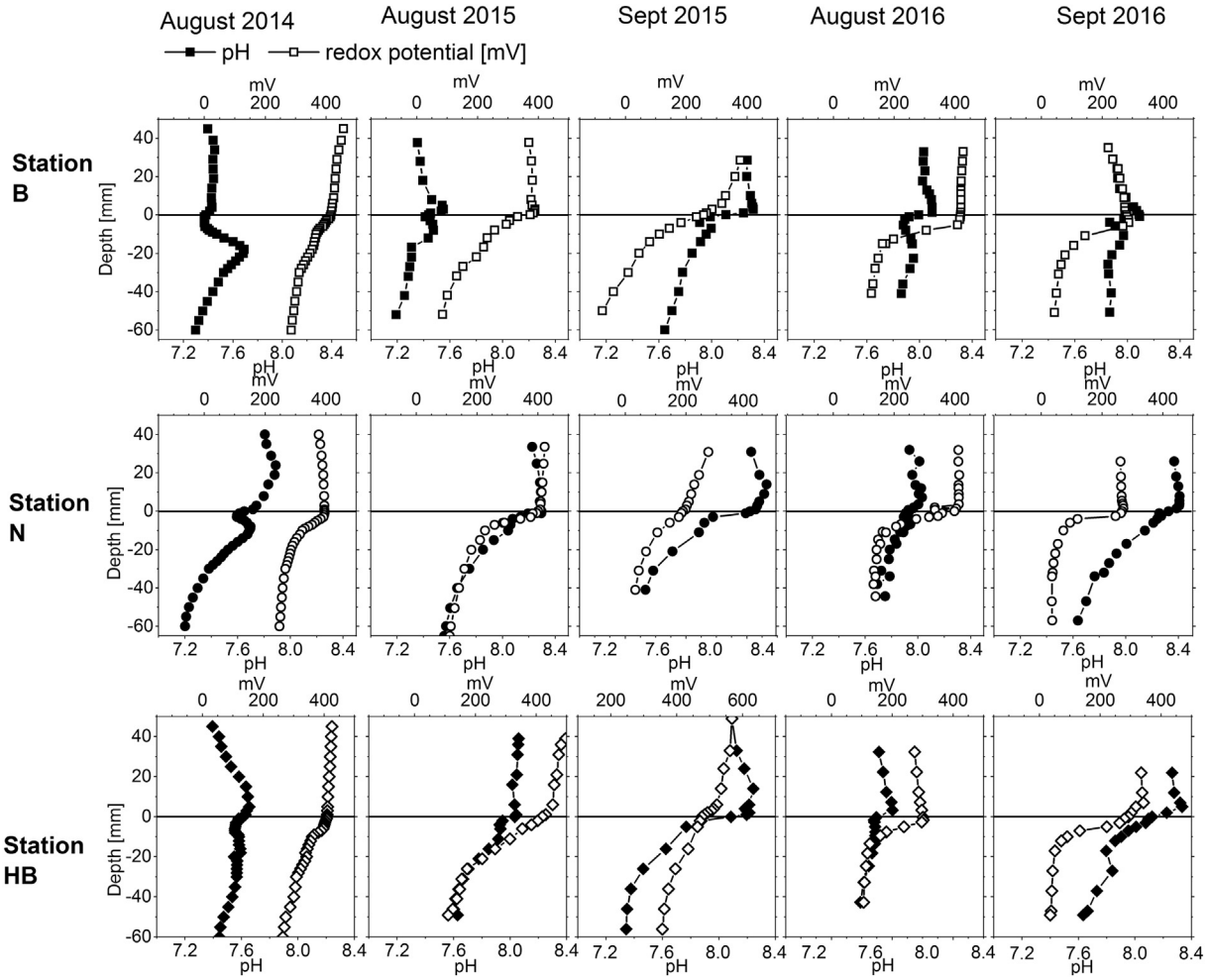

Fig. 2. The pH and redox potential profiles at the sediment-water interface: station B (top row), station N (middle row) and station HB (bottom row).

where $\Sigma\Delta C_i$ represents the sum of differences between the measured P distributed in different binding forms at stabilization depth and each layer i above it, ρ_i is dry bulk density, and x_i represents the thickness of each layer. We performed this calculation for all P fractions by substituting the sum of the fractions with concentrations of a particular fraction, and thus identified the P binding forms that contribute to P release and represent the mobile P pool.

2.10. Short-term and long term P release calculation

In this study, sediment P fluxes were calculated using two independent methods: (i) short-term P release which reflects pore water diffusive flux (J_{SRP}), calculated using Fick's first law, and (ii) long-term P release assessed from concentrations of sediment P binding forms and the known age-depth relationship (e.g., Hupfer and Lewandowski, 2005). The former method represents in situ P release at the time of sampling and reflects seasonal and spatial variations of physical and biogeochemical processes (e.g., Lewandowski et al., 2002; Lewandowski and Hupfer, 2005). On the other hand, the release rate calculated using the second method represents long-term multi-seasonal recycling of sedimentary P.

The SRP diffusive flux was calculated from concentration gradients across SWI using Fick's first law (Berner, 1980):

$$J_{SRP} = D_{sw}\frac{\varphi}{\theta^2}\frac{\partial C}{\partial x} \quad (2)$$

where φ is the porosity, ∂C represent SRP concentration, $\partial C/\partial x$ represent concentration gradient in the depth interval over which gradient is calculated (uppermost 1-2 cm), and θ represents the tortuosity, or the degree of deviation around particles; θ^2 factor was calculated using the empirical relationship $\theta^2 = 1 - ln(\varphi^2)$, where φ is porosity (after Boudreau, 1997), and D_{sw} is a molecular diffusion coefficient of PO_4 in the pore water, assuming ambient hypolimnion temperature (values after Boudreau, 1997).

While diffusive flux calculation based on Fick's first law does not account for a number of factors affecting sediment P fluxes, including advection and bioturbation, the diffusive P release fluxes are an important tool for the estimation of internal loading, and have been used in a number of studies (e.g., Dittrich et al., 2013; Tammeorg et al., 2015).

To constrain the long-term P dynamics we also estimated gross P release rates using the difference between P accumulation at the sediment surface and P burial at its stabilization depth (e.g., Rydin et al., 2011; Dittrich et al., 2013). This difference between surface and deep sediments reflects the pool of temporary stored sediment P and extent of long-term P retention, which is controlled by sediment biogeochemical and mineralogical composition, accumulation and diagenesis. Sediment composition and accumulation also reflect local tributary inputs, watershed geology and land-use patterns, which are often site and lake specific (e.g., Dittrich et al., 2013).

The accumulation rate of P was estimated from bulk sediment accumulation and P concentration in the surface layer. The P burial was calculated using the sedimentation rate and P concentration at the stabilization depth. The average P release rate was calculated by subtracting the burial of P from estimated P accumulation (e.g. Hupfer and Lewandowski, 2005; Rydin et al., 2011; Dittrich et al., 2013; Puttonen

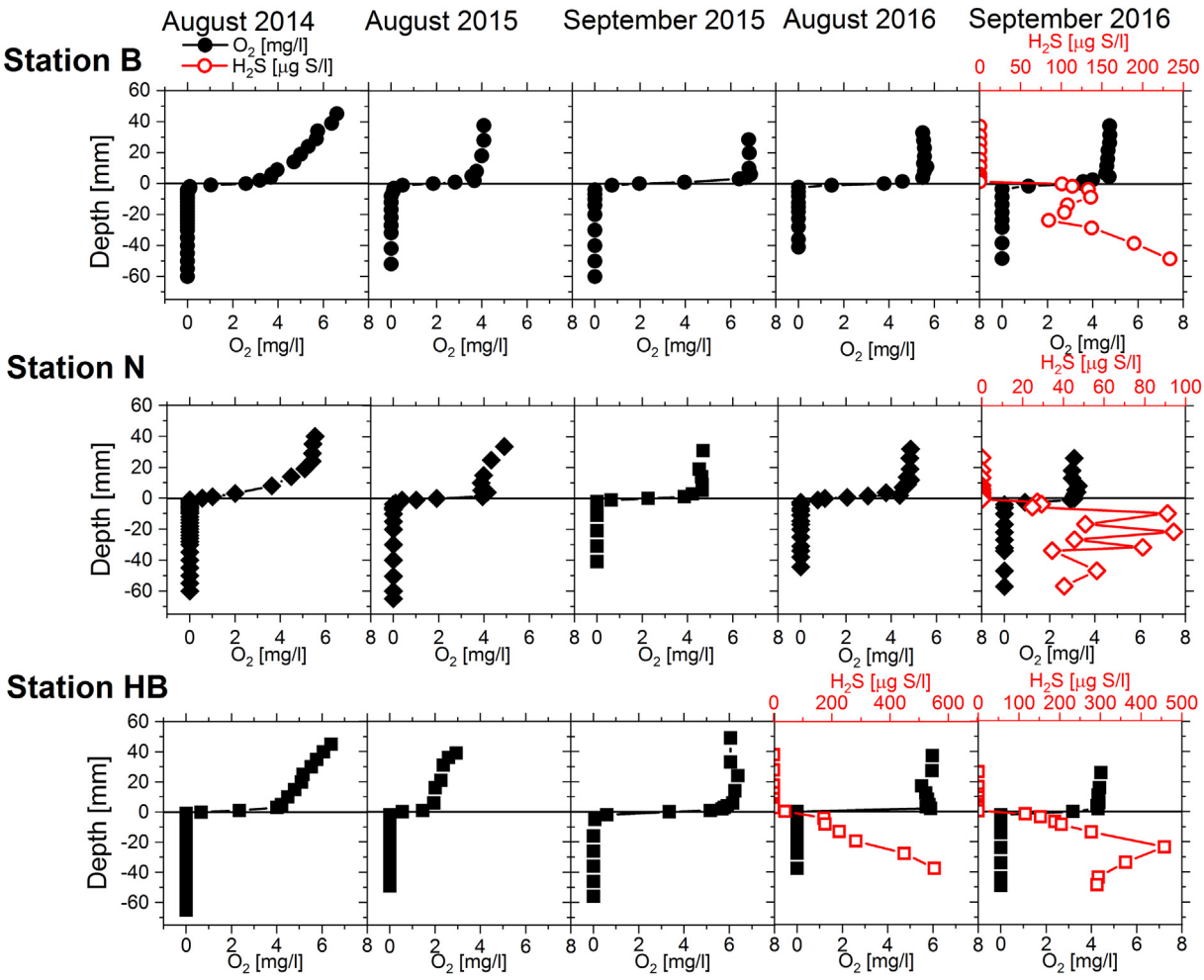

Fig. 3. DO and H_2S concentrations at the sediment-water interface: station B (top row), station N (middle row) and station HB (bottom row).

et al., 2014). In the same manner, P release was calculated for each fraction to identify the P binding forms that contribute to release, burial or both.

$$P_{release} = C_0 \times U_0 - C_s \times U_s \quad (3)$$

where C_0 and C_s represent P concentration (expressed as mg/g in sediment dry weight) in the topmost layer and at the stabilization depth, respectively (for each fraction as well as the sum of them), while U_0 and U_s represent the dry sediment accumulation rate (in units g/cm^2/yr) at the sediment surface and burial rate at the stabilization depth, respectively.

In addition, we estimated the intra-basin P retention capacity (or burial efficiency) using the ratio between P release and burial rate obtained from the sediment P depth profiles and estimated sediment accumulation rates (Ingall and Jahnke, 1994).

2.11. Calculation of mineralization rates

The degradation of organic matter in sediments proceeds through a variety of microbial processes, arranged as a “redox cascade” of reactions with decreasing energy yield (e.g., Burdige, 2006). Oxygen is the preferred oxidant, used simultaneously in aerobic organic matter degradation and also in the oxidation of reduced products of anaerobic organic matter degradation processes (e.g. manganese, iron or sulfate reduction). Hence, O_2 is the ultimate electron acceptor, and sediment oxygen uptake has often been used as a proxy for total organic matter degradation (e.g., Jørgensen, 1982; Maerki et al., 2009; Li et al., 2012).

Oxygen uptake, however, does not account for processes that produce inert compounds such as the denitrification of nitrate to inert dinitrogen, or processes that permanently bind a portion of reduced metabolic by-products such as the diagenetic precipitation of iron sulfides. Denitrification is typically limited by concentrations of $NO_3 + NO_2$, which are generally low in the Bay of Quinte, reaching values near the detection limit toward the end of summer (Currie and Frank, 2015). Thus, we can assume that the denitrification pathway plays a minor role in the total sediment carbon mineralization in this waterbody. Similarly, as sulfate reduction in freshwater sediments is restricted by the low sulfate concentrations, the relative contribution of sulfate reduction and organic matter degradation due to iron sulfide precipitation of can be assumed to play relatively minor role.

Sediment oxygen uptake was calculated from O_2 concentration gradient across SWI using Fick's first law:

$$J_{O2} = D_{sw} \frac{\varphi}{\theta^2} \frac{\partial C}{\partial x} \quad (4)$$

where φ is the porosity, ∂C is the O_2 concentration, ∂x depth interval over which gradient is calculated (exact depth varied between 1 and 3 mm), θ represents the tortuosity, or the degree of deviation around particles; θ^2 factor was calculated using the empirical relationship $\theta^2 = 1 - ln(\varphi^2)$ (after Boudreau, 1997), and D_{sw} is a molecular diffusion coefficient of O_2 in the pore water, assuming ambient hypolimnion temperature (values after Boudreau, 1997).

Similarly, diffusive fluxes of NH_4^+, SO_4^{2-}, reduced iron and manganese were calculated from their respective measured concentration gradients in pore water. The depth interval used for calculation of concentration gradient was the top 1-2 cm. Diffusion coefficients for

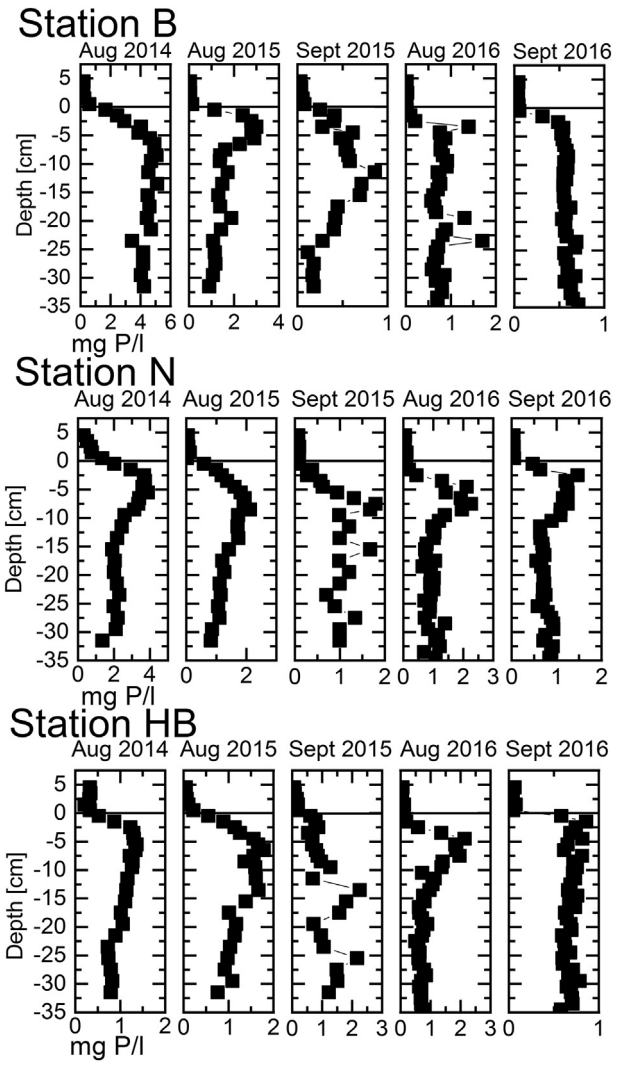

Fig. 4. Pore water SRP concentration across the sediment-water interface: station B (top), station N (middle) and station HB (bottom).

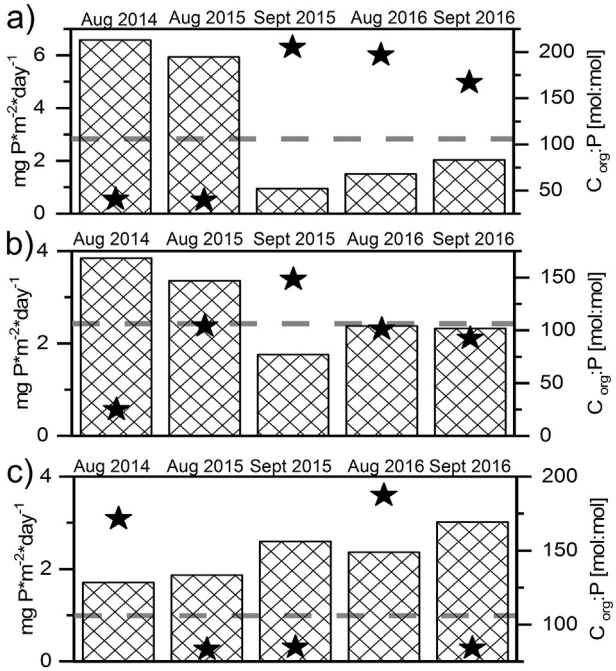

Fig. 5. Diffusive P fluxes (column) and the ratio between organic carbon degradation and phosphorus release (mol:mol) from sediments (stars): (a) station B, (b) station N and (c) station HB.

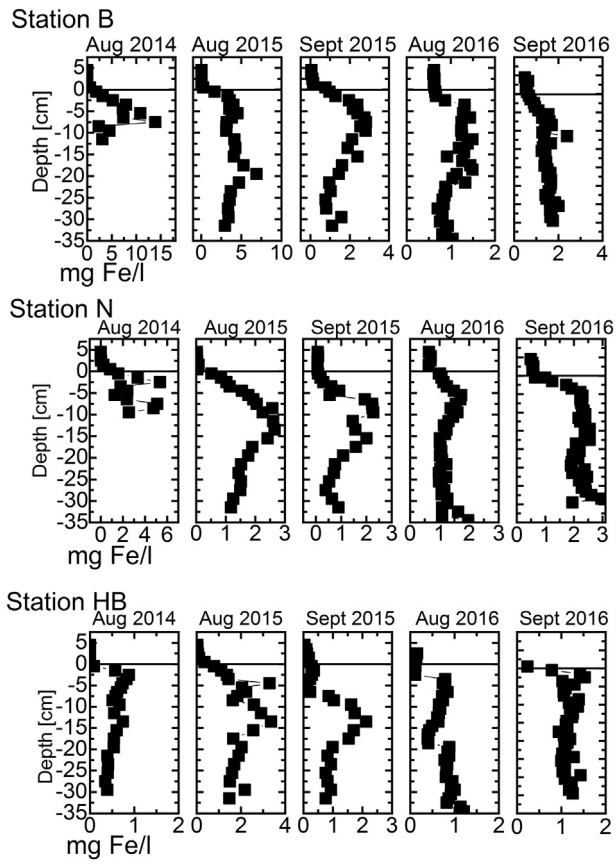

Fig. 6. Concentrations of Fe in the water overlaying sediments and pore water: (a) station B, (b) station N and (c) station HB.

respective ions correspond to ambient temperature freshwater estimates after Boudreau (1997).

Sediment oxygen uptake reflects the total organic matter mineralization rate and represents the sum of denitrification (R_{denit}), oxic (R_{oxic}) and anoxic (R_{anoxic}) pathways (Maerki et al., 2009):

$$R_{total} = R_{oxic} + R_{denit} + R_{anoxic} \quad (5)$$

Due to low lake water $NO_3 + NO_2$ concentration in the Bay of Quinte (Currie and Frank, 2015), the denitrification mineralization pathway likely plays a minor role in the total sediment carbon mineralization, which is assumed to be equal to the oxygen uptake, while the contribution of specific mineralization pathway was calculated as a product of diffusive fluxes and the relevant stoichiometric factors of the particular metabolic reaction described elsewhere (Burdige, 2006; Maerki et al., 2009):

$$R_{total} = J_{O2} = R_{oxic} + R_{anoxic} \quad (6)$$

$$R_{anoxic} = \frac{1}{4} \times J_{Fe^{2+}} + \frac{1}{2} \times J_{Mn^{2+}} + 2 \times J_{SO_4^{2-}} + 2 \times J_{CH_4} = \varepsilon_{C:N} \times J_{NH_3} \quad (7)$$

where $\varepsilon_{C:N}$ represents the measured molar ratio of organic C:N in the surface sediment (upper 2 cm) and used to estimate total anaerobic organic matter mineralization (Maerki et al., 2009), and J_{Fe}^{2+}, J_{Mn}^{2+}, J_{SO4}^{2-}, J_{CH4}, J_{NH3} are fluxes of iron (II), manganese (II), SO_4^{2-}, methane and NH_4^+. Note that the calculated oxygen uptake and fluxes of other solutes should be considered minimum estimates, as they are likely lower than actual rates, because diffusion is assumed as the sole

Table 1
Sediment oxygen uptake, fluxes of Mn^{2+}, Fe^{2+}, SO_4^{2+}, NH_4^+ and organic matter degradation rate (anaerobic and total).

Station	J_{O2} (Stand. Dev.)	J_{Mn}^{2+}	J_{Fe}^{2+}	J_{SO4}	J_{NH4}	POC:PON	Average $R_{anaerobic}$**	R_{total}
		[mmol ∗ m^{-2} ∗ d^{-1}]					[mmol C ∗ m^{-2} ∗ d^{-1}]	
B	8.7 (2.5)	−0.127 (0.048)	−0.068 (0.061)	0.293–0.564	0.451–1.223	8.3	3.74–10.1	8.7 ± 2.5
N	7.8 (3.1)	0.076 (0.054)	−0.050 (0.018)	0.441–0.484	0.586–0.831	8.2	4.80–6.81	7.8 ± 3.1
HB	8.8 (3.5)	0.033 (0.002)	−0.031 (0.015)	0.595–0.881	0.785–0.791	9.5	7.51–7.57	8.8 ± 3.5

Table 2
P accumulation and retention. Note that potentially mobile P is assumed to be a sum of NH_4Cl-P, BD-P, NaOH-SRP, NaOH-NRP (Fig. 9).

Site	$P_{accumulation}$ [g/m^2/yr]	P_{burial} [g/m^2/yr]	Retention total P [%]	Potentially mobile $P_{accumulation}$ [g/m^2/yr]	Potentially mobile P retention [%]
Station B	1.31 (± 0.25)	0.74 (± 0.07)	58 (± 13)	0.92 (± 0.22)	41 (± 7)
Station N	1.26 (± 0.24)	0.76 (± 0.05)	62 (± 13)	0.96 (± 0.18)	35 (± 13)
Station HB	1.69 (± 0.48)	0.98 (± 0.06)	61 (± 15)	1.2 (± 0.34)	39 (± 7)

transport process. In shallow water bodies like the Bay of Quinte, oscillating redox conditions due to physical mixing of sediments likely contribute significantly to the transport of oxygen and dissolved substances across the sediment-water interface (Aller, 1994).

2.12. Statistical analysis and geochemical speciation modelling

The relationships between P and metals measured in P binding pools were assessed using scatter matrix plots, and pairwise Pearson correlation coefficients. A two-tail test of significance was used, and correlation significance was assessed at the 0.05 level. Results significant at these P values are highlighted. Calculations were performed using software Origin 2017.

The saturation state of apatite ($Ca_5(PO_4)_3(OH)$) and vivianite ($Fe_3(PO_4)_28(H_2O)$) in lake water and pore water ion activities and saturation indices were calculated from measured water chemistry, pH and redox potential using PHREEQC version 3 (Parkhurst and Appelo, 2013). Estimation of pore water saturation state with respect to minerals (apatite and vivianite) was carried out assuming the equilibrium of solution species at an ambient temperature of 20 °C.

3. Results

3.1. The pH, redox potential, DO and H_2S at SWI

At all stations, the pH values in the overlying water and sediment were circumneutral to slightly alkaline (Fig. 2). The general decreasing trend from the overlying water toward sediment was interrupted by the distinct pH peaks, present at or near the SWI. These transient peaks were followed by a monotonic decrease with depth.

The redox potential (Eh) in the overlying water was between 200 mV and 600 mV and decreased rapidly below SWI, reaching minimum values of 0–100 mV at 5–6 cm below SWI. The lowest Eh values were in September 2015 at stations B and N (−100 mV and 50 mV, respectively), while comparable minimum values at station HB were observed in August 2015 and 2016 and September 2016.

DO concentrations in the water overlying sediment were in the range of 2–6 mg O_2/l. Thus, bottom water was overall oxygenated except for the August 2015 measurement at station HB, which met the criteria for hypoxia (DO < ~2 mg O_2/l). All stations DO show very steep gradients across SWI with sediment anoxia below 2–3 mm (Fig. 3 and Fig. S2). These steep concentration gradients led to high oxygen uptake (8–13 mmol/m^2/d, 3–11 mmol/m^2/d and 7–14 mmol/m^2/d at stations B, N and HB respectively, Fig. S2).

Total sulfide was measured during summer 2016. In August 2016, sulfide was detected at SWI at a single station, HB, where it increased rapidly with sediment depth to a maximum concentration of 528 µg S/l. In September 2016, sulfide was detected at all stations, with concentrations again increasing with depth up to 224, 92 and 480 µg S/l at stations B, N and HB, respectively.

3.2. Pore water SRP and diffusive P fluxes

At all stations, the SRP concentrations in the overlying lake water ranged between 0.02 and 0.2 mg P/l (Fig. 4). Interstitial SRP concentrations at station B increased rapidly with sediment depth to 0.8–5.1 mg P/l. In August and September 2015, this increase was followed by a reverse trend below 6 cm and 12 cm, respectively. The benthic diffusive P fluxes showed considerable temporal variability, with the highest values in August 2014 and August 2015 (6.5 mg P/m^2/d and 5.9 mg P/m^2/d, respectively) and the lowest values in September 2015 (1 mg P/m^2/d) (Fig. 5).

From minima at the SWI, the pore water SRP concentrations increased rapidly with depth up to 3.7 mg P/l (August 2014) at station N, followed by a decrease with depth (Fig. 4). The benthic P fluxes were highest in August 2014 and August 2015 (3.8 mg P/m^2/d and 3.4 mg P/m^2/d, respectively), while the lowest values were in September 2015 (1.8 mg P/m^2/d) (Fig. 5).

The pore water SRP concentrations at the deepest station HB were markedly lower than at the other two stations, with a maximum SRP of 2.2 mg P/l measured in September 2015 (Fig. 4). Following a positive gradient in the topmost 10 cm, SRP concentrations were fairly constant with depth, except in August 2015 and August 2016, when a decrease with depth was observed. The temporal variability of benthic P fluxes was also considerably smaller at HB compared to the other two stations, with maximum and minimum SRP fluxes of 1.8 mg P/m^2/d and 3.0 mg P/m^2/d in August 2014 and September 2016, respectively (Fig. 5).

The ratios between SRP release and organic matter degradation rates (estimated using oxygen uptake) were used to calculate the C:P flux ratios (Fig. 5). In August 2014 and 2015 at station B, August 2014 at station N and August 2015 and September 2015&2016 at station HB, these ratios were 2–3 lower than the Redfield ratio (molar ratio C:P = 106, Redfield et al., 1963), which would be expected if organic matter was the sole pool of P. On other dates, the ratios were close to the Redfield value or higher (up to 200).

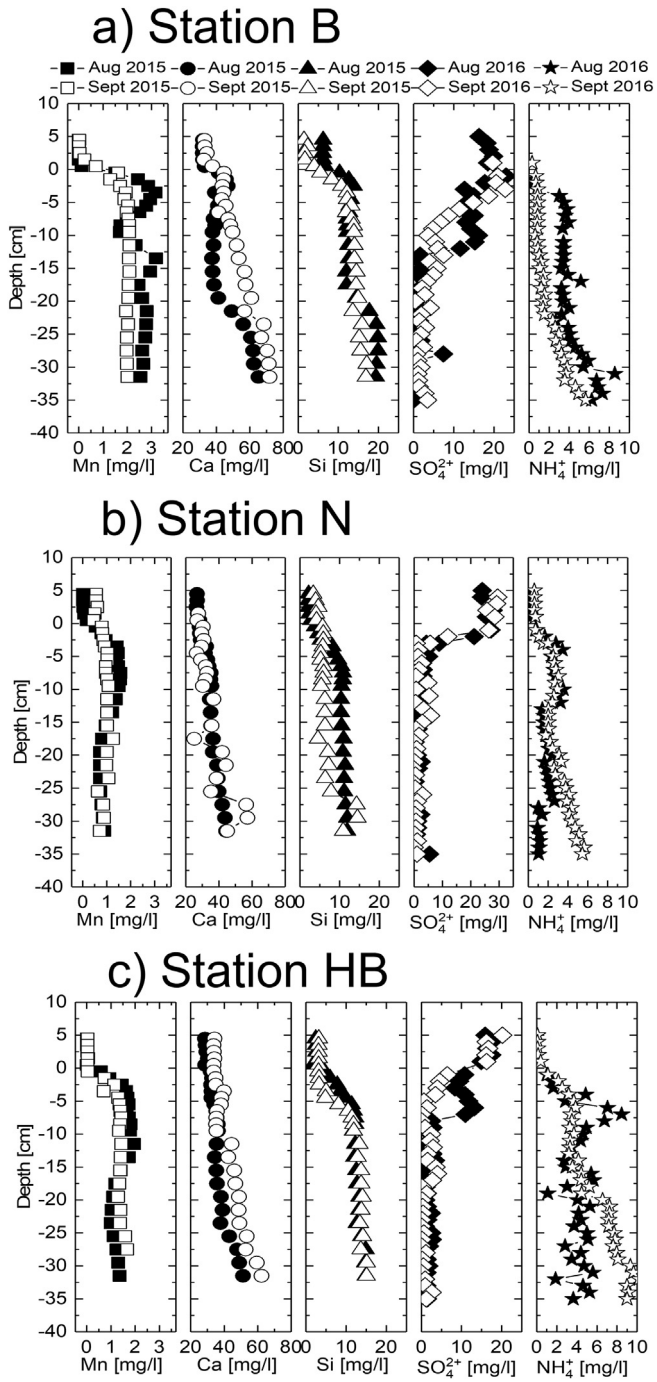

Fig. 7. Concentrations of Mn, Ca, Si, SO_4 and NH_4 in the water overlaying sediments and pore water (August and September 2015–2016): (a) station B, (b) station N and (c) station HB.

3.2.1. Pore water chemistry and organic matter mineralization rates

Below SWI, Fe^{2+} increased rapidly with the lowest values present in the top 1 cm (0.6–1.8 mg Fe/l, 0.5–1.5 mg Fe/l and 0.09–0.7 mg Fe/l, at stations B, N and HB, respectively, Fig. 6). The overall highest concentrations were measured at station B (up to 14 mg Fe/l in August 2014), while at stations N and HB the maximum values were 5 mg Fe/l and 3 mg Fe/l, respectively (Fig. 6).

The pore water Fe:SRP ratios, which reflect the sediment's capacity to retain P (Smolders et al., 2001), were generally < 1, with the exception of the topmost layers (top 1–3 cm), where they reached up to 30 (August 2016) (Fig. S3). These sharp shifts of Fe:SRP ratios near the SWI are indicative of rapid Fe oxidation and P sorption on iron oxyhydroxides. The flux of Fe^{2+} across SWI at station B varied between 0.7 mg Fe/m^2/d and 7.7 mg Fe/m^2/d compared to 1.1–4.2 mg Fe/m^2/d and 0.5–2.5 mg Fe/m^2/d at stations N and HB, respectively (Fig. S3).

Organic matter degradation rates were calculated from sediment O_2 uptake using DO measurements (Table 1; see Table S3 for individual dates) and were on average 8.7, 7.8 and 8.8 mmol C/m^2/d at stations B, N and HB, respectively.

3.3. Phosphorus binding forms

At station B, the average total P decreased with depth from 1.84 ± 0.29 mg/g P d.w. in the surface sediments to 1.34 ± 0.29 mg/g P in the deepest layer (Fig. 8c). The dominant binding forms in the surface sediments were HCl-P and redox-sensitive BD-P, which contributed on average 28% and 25%, respectively (Fig. 8b). The relative contribution of HCl-P increased downcore to 44% in conjunction with the decline of the BD-P to 17%–20% in the deepest sediment layers (Fig. 8j).

The average total P at station N decreased downcore from 1.71 ± 0.30 mg/g P d.w. in the surface sediments to 1.30 ± 0.30 mg/g P d.w. in the deepest layer (Fig. 8f). The dominant binding forms in the surface sediments were BD-P and NaOH-SRP with 28% and 27% of the total P, respectively (Fig. 8k). The relative proportion of redox-sensitive P decreased downcore from a maximum in the surface sediments of 28% to a minimum of 13% of the total P in the deepest sediment layer (Fig. 8k). At the same time, the relative content of HCl-P grew from 24% of the total P in the surface sediments to 45% in the deepest sediment layer (Fig. 8k).

Station HB showed the lowest average total P among the three areas. The P content decreased with depth from 1.56 ± 0.40 mg P/g d.w. in the surface sediments to 1.17 ± 0.11 mg P/g d.w. in the deepest sampling interval (Fig. 8i). The redox-sensitive BD-P was the most abundant binding form in the surface sediments, accounting for 30% of the total P, closely followed by NaOH-SRP and Ca-bound HCl-P, which both represented 22% of the total P on average (Fig. 8l). The redox-sensitive P and NaOH-SRP decreased with depth from the highest concentrations in the surface sediments (0.47 ± 0.20 mg P/g d.w. and 0.35 ± 0.12 mg P/g d.w, respectively) to a minima in the deepest sampled intervals (0.23 ± 0.02 mg P/g d.w and 0.15 ± 0.04 mg P/g d.w., respectively) (Fig. 8h). The contribution of HCl-P increased downcore to a maximum of 45% of the total P (Fig. 8l).

The average molar ratios of organic C (see Fig. S4 and Fig. 8) to organic P (defined here as a sum of NaOH-NRP and Ref-P fractions) were consistently well above the theoretical Redfield ratio of 106 (Fig. 8c; f; i). At station B, the ratio varied between 750 and 850, while at stations N and HB it ranged between 650 and 1500, and 650 and 1200, respectively (Fig. 8c; f; i).

3.3.1. Long term P release rates and diagenetically mobile P

Using the sedimentation rates (Fig. S5) and depth profiles of different P pools (Fig. 8), we estimated the potentially mobile P pool and gross retention/release rates. Mobile P varied between 3.5 g/m^2 at station N and 4.7 and 5 g/m^2 at stations HB and B. Binding forms that constituted this pool include NH_4Cl-P, BD-P, NaOH-NRP and NaOH-SRP at stations B and HB, while at station N, contribution from NaOH-NRP was minor compared to BD-P and NaOH-SRP (Fig. 9a).

The estimated rates of P release were similar at the two upper sites, but they were significantly higher in the lower bay (1.5, 1.54 and 1.95 mg P/m^2/d at stations B, N and HB, respectively; Fig. 9b). BD-P fraction was the dominant binding form driving P release at all stations, followed by NaOH-NRP at station B, and NaOH-SRP at stations N and HB. At the same time, P immobilization due to Ca-bound P formation was 0.05, 0.16 and 0.17 mg P/m^2/d at stations B, N and HB, respectively (Fig. 9).

The ratios of P burial vs. P accumulation (burial efficiency or retention) at stations B, N and HB were 58%, 62% and 61%, respectively

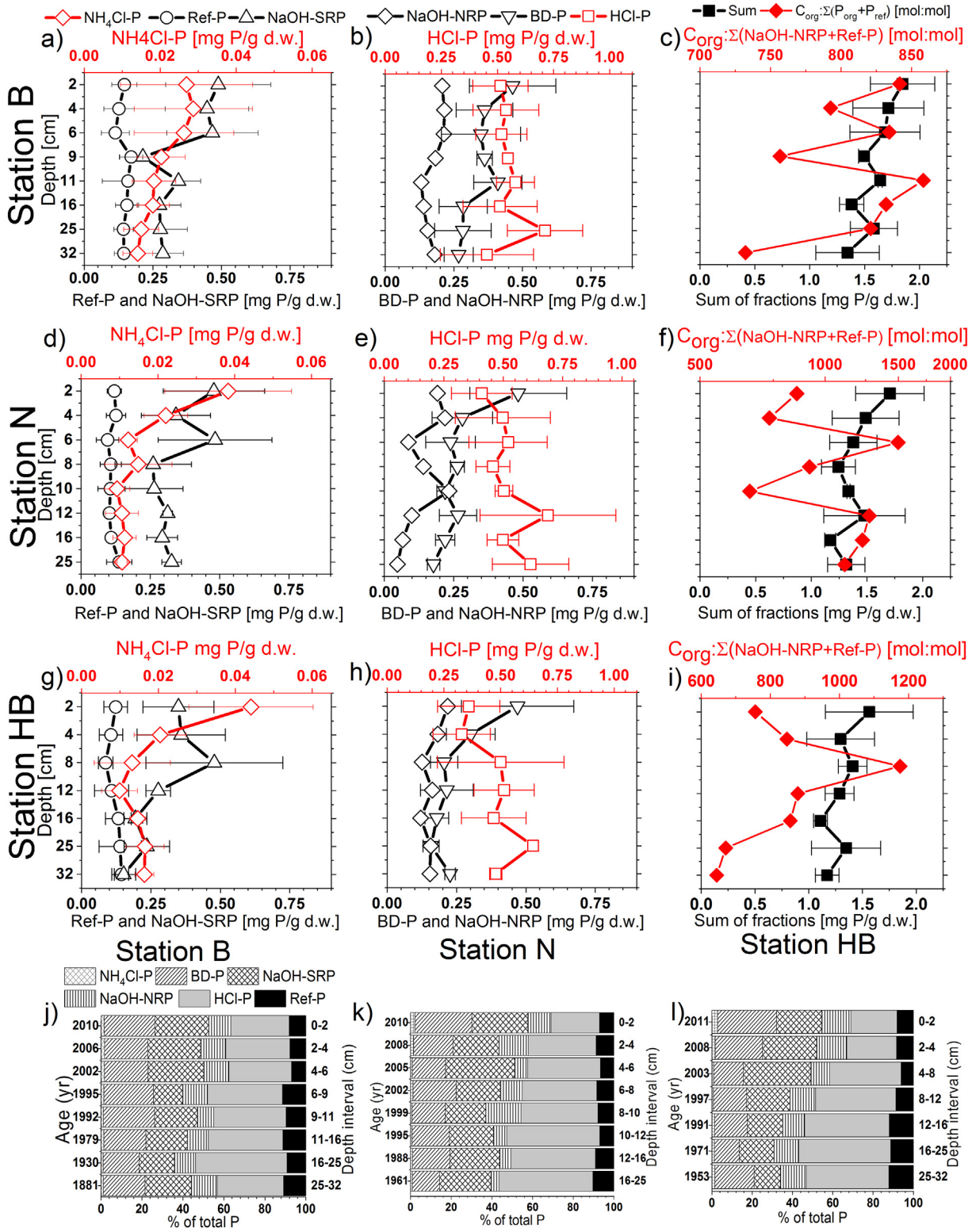

Fig. 8. P fractions – all sampling dates (2013–2015). Average concentrations of P binding forms at station B (a, b, c), station N (d, e, f) and station HB (g, h, i) and their relative distribution at station B (j), station N (k) and station HB (l). The molar ratio of organic carbon to organic P (defined as sum of P_{org} and P_{ref} binding pools): station B (c), station N (f) and station HB (i).

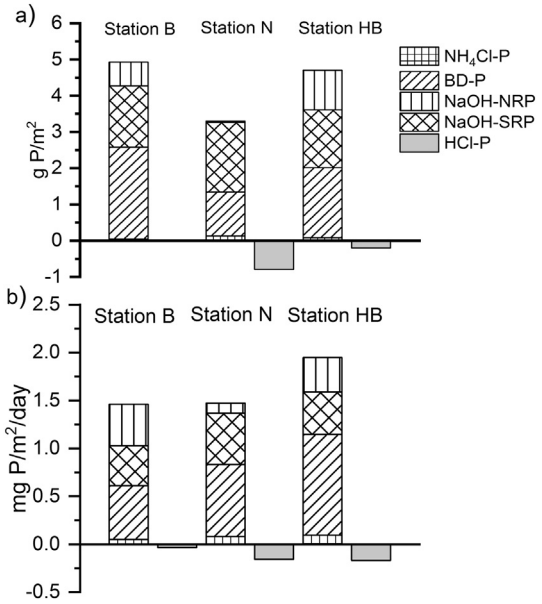

Fig. 9. Potentially mobile P in sediment (a) and P release (b). Note that P release is calculated as a daily rate to facilitate comparison with the diffusive fluxes presented in the following section.

(Table 2). The retention ratio for potentially mobile P (NH_4Cl-P, BD-P, NaOH-NRP and NaOH-SRP) was even lower with the values of 35%–40% (Table 2).

4. Discussion

4.1. Short- and long-term P release rates: the role of basins depths, land use and benthic organisms

Overall, the results of this study provide important insight into P sediment geochemistry in shallow eutrophic lake, which have implications not only for P cycling in the Bay of Quinte, but to many other shallow systems with a history of eutrophication. Short-term summer diffusive fluxes obtained from pore water SRP concentration gradients were 3.6 ± 2.5 mg P/m^2/day, 2.7 ± 0.8 mg P/m^2/day and 2.3 ± 0.5 mg P/m^2/day for stations B, N and HB, respectively. Manning (1996) estimated a diffusive P flux from the Upper Bay (station B) of 1.34 mg P/m^2/day using pore water depth profiles from September 1988 and 1989, while Sly (1990) estimated a flux of 9.3 mg P/m^2/day using benthic chamber measurements collected in summer 1987. Almost three decades later, our data indicate that benthic P fluxes are still within the same order of magnitude.

In many shallow lakes, pore water SRP concentrations increase rapidly and sustain elevated diffusive P fluxes following deposition of organic matter originating from recent phytoplankton blooms (Tammeorg et al. 2015 & 2016). Degradation of freshly deposited biomass decreases redox potential in surface sediment below critical value of 200 mV which is thought to mark iron reduction zone and coincide with the release of P adsorbed on ferric oxyhydroxides (Tammeorg et al. 2015 & 2016). Furthermore, low redox potential and anoxic conditions in surface sediment can stimulate microbial release of polyphosphate, which in some lakes may account for large portion of total P in sediment (Hupfer et al., 2004). In our dataset, redox potential reached values below 200 mV in the top 2 cm except in August 2014 (at all three stations) and September 2015 (station HB) (Fig. 2). High diffusive fluxes persisted also on sampling dates where surface sediment redox potential was above 200 mV (Fig. 5). On those dates it is possible that sampling was conducted during resuspension events, with mixed or bioturbated surface sediment, which can temporarily increase SRP

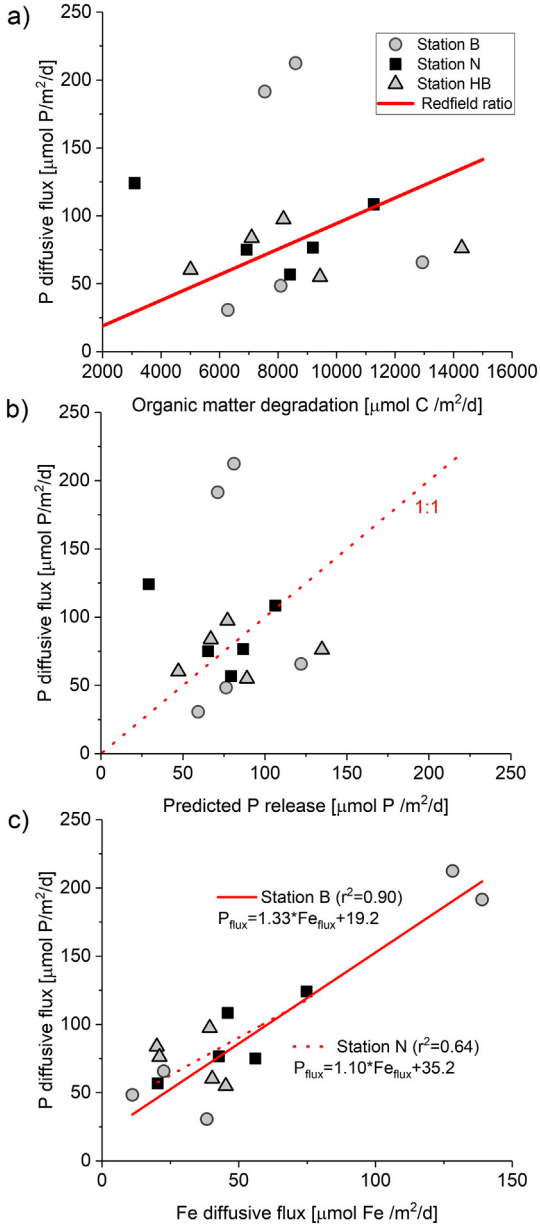

Fig. 10. Organic matter degradation rates versus P diffusive fluxes (a); P release predicted (using $P_{pred} = R_{total}/106$) and P fluxes (b); diffusive fluxes of iron and phosphate (c).

concentrations gradients, thereby increasing diffusive P fluxes, while at the same time redox potential in physically mixed surface sediments remains elevated as has been shown by Tammeorg et al. (2015 & 2016).

Short-term diffusive P release indicates seasonal contribution of sediment P recycling to the lake budget which are very sensitive to changes of physicochemical conditions (O_2, pH and Eh), sediment mixing and fresh sediment supply to the sediment water interface (Jensen and Andersen, 1992; Katsev et al., 2006; Lewandowski et al., 2007; Smith et al., 2011; Tammeorg et al. 2015 & 2016; Parsons et al., 2017). Consequently, short-term P fluxes are not representative of the long-term sediment P retention and release potential (Katsev et al., 2006). On the other hand, the long-term P release (Fig. 9; 1.5, 1.54 and 1.95 mg P/m^2/d at stations B, N and HB, respectively) are indicative of the long-term potential of sediment to release P. The long-term release rates represent combined effect of multiple processes of sediment P mobilization and diagenetic P transfers from labile to more stable solid P forms integrated over periods of several years to decades. For

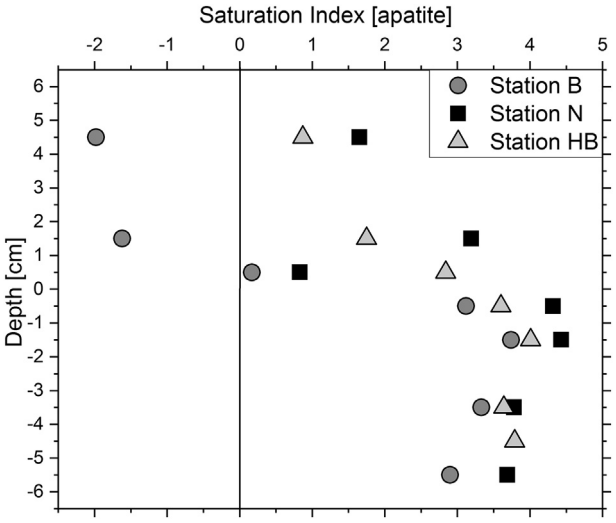

Fig. 11. Saturation indices (SI) of apatite in lake water and surface sediments (August 2015 sampling). SI < 0 indicates undersaturation, SI > 0 indicates supersaturation, and SI = 0 indicates equilibrium with respect to apatite. Speciation calculations were performed using PHREEQC (Parkhurst and Appelo, 2013).

instance, while temporal decrease of redox potential at SWI supports release of P sorbed iron oxyhydroxides, a large proportion of mobilized P is redistributed vertically within sediments and remains bound to mineral phases (e.g., Wilson et al., 2010; Parsons et al., 2017). Solid sediment P profiles and binding forms reflect these diagenetic transformations and P deposition history, including changes of external loading and land-use patterns (e.g., Hupfer and Lewandowski, 2005; Dittrich et al., 2013). Hence, long-term P release represents the base potential for sediment P mobilization, which reflects long-term trends of P accumulation and burial. The size and mobility of sedimentary P pool is essential for water quality management and needs to be considered in order to devise successful and sustainable P management strategy and watershed P reduction targets.

At stations B and N, short-term diffusive P release was twice as large as that of long-term diagenetic P release. This can be interpreted as a short-term summer pulse of increased mobilization of labile P forms (redox sensitive BD-P, organic P forms from fresh algal debris, e.g. polyphosphate) in response to environmental conditions and phytoplankton dynamics, similar to observations in other shallow systems like lake Peipsi (Tammeorg et al., 2015) and Cootes Paradise (Parsons et al., 2017). In contrast to stations B and N, short-term diffusive P fluxes at the deeper station HB were only ~20% higher than long-term P release estimated from sediment P profiles. This difference can be interpreted in terms of basin depth and benthic community. As station HB is considerably deeper than the two stations in the upper bay, settling algal debris likely has more time to decay before reaching lakebed. If this is true, at station HB, a substantial portion of labile P is likely to be recycled in the water column before reaching sediment. In contrast, stations B and N are shallow, with lakebed colonized by dreissenid mussels (Nicholls et al., 2011). Filter feeding dreissenids can affect particle deposition and P recycling through the ingestion of algal and other debris and subsequent deposition of particles as faeces and pseudofaeces (Howell et al., 1996; Ozersky et al., 2013; Mosley and Bootsma, 2015). Manning (1996) showed that before dreissenid colonization in the mid-90s a large proportion of suspended particles from upper basins of the Bay of Quinte was exported downstream to Hay Bay. While there are no recent estimates, Bailey et al. (1999) concluded that their filtration capacity (0.1–10 days) far exceeded water renewal time, effectively intercepting suspended algal particles and accelerating their deposition - increasing carbon and P content of surrounding surface sediment of the upper bay sites. At the same time, mussel respiration

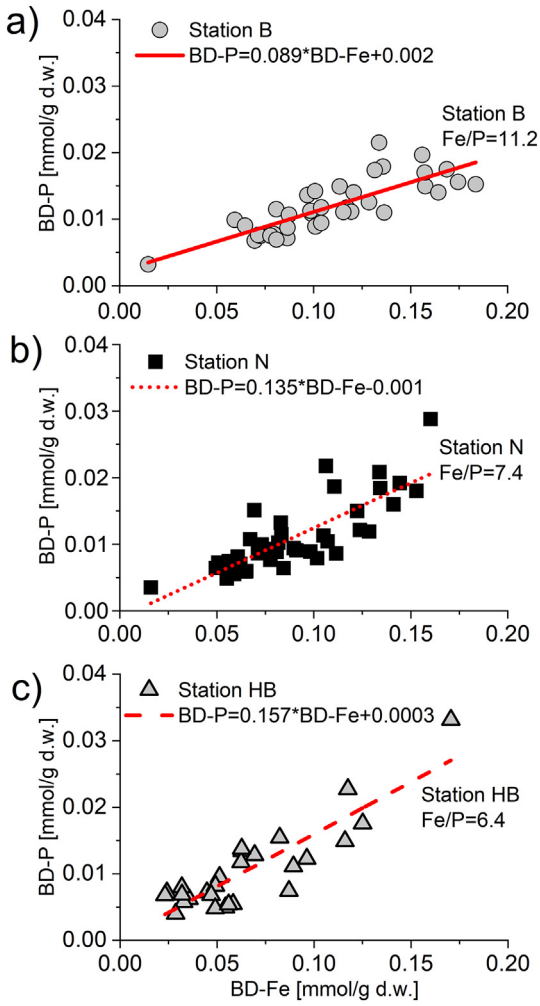

Fig. 12. Molar ratio between reducible Fe and associated P: (a) station B, (b) station N and (c) station HB. Molar Fe:P ratio is lower than 6.7, suggesting the supersaturation of surface binding sites of ferrihydrite (Sigg and Stumm, 1981) or the coprecipitation of metastable P-ferrihydrate assemblage, which has maximum Fe:P ratio of 2:1 (Thibault et al., 2009), or both.

depletes oxygen near lake bed (Ozersky et al., 2013) while their guts and excreta represent anaerobic environments (Hecky et al., 2004), affecting the cycling of redox sensitive elements. In turn, this may mobilize redox sensitive P forms in surface sediment and likely contributes to higher short-term diffusive P fluxes at stations B and N.

The Bay of Quinte system is shallow, and frequent wind-generated mixing results in well oxygenated bottom waters at stations B and N during illuminated periods (Currie and Frank, 2015). Well oxygenated bottom waters are thought to preserve oxidized ferric microlayer at the sediment interface which acts as a sorptive barrier for diffusive P flux (Mortimer, 1942). However, considerable short-term diffusive fluxes of dissolved P were found during study period, despite oxygenated bottom water throughout most of the sampling dates (Fig. 3). Temporary bottom water hypoxia and anoxia can potentially develop on a diurnal basis, as a result of O_2 depletion at night due to the sediment respiration in the absence of photosynthesis and have been observed at the deeper station HB (Currie and Frank, 2015; also during August 2015 in our dataset), which could potentially increase anaerobic P mobilization. However, short-term diffusive fluxes at this station were not higher during sampled hypoxic periods, suggesting that hypoxia does not play a major role in short-term P mobilization at this site. This is consistent with recent reassessments of the role of hypolimnetic oxygen levels (Katsev et al., 2006; Hupfer and Lewandowski, 2008; Katsev and

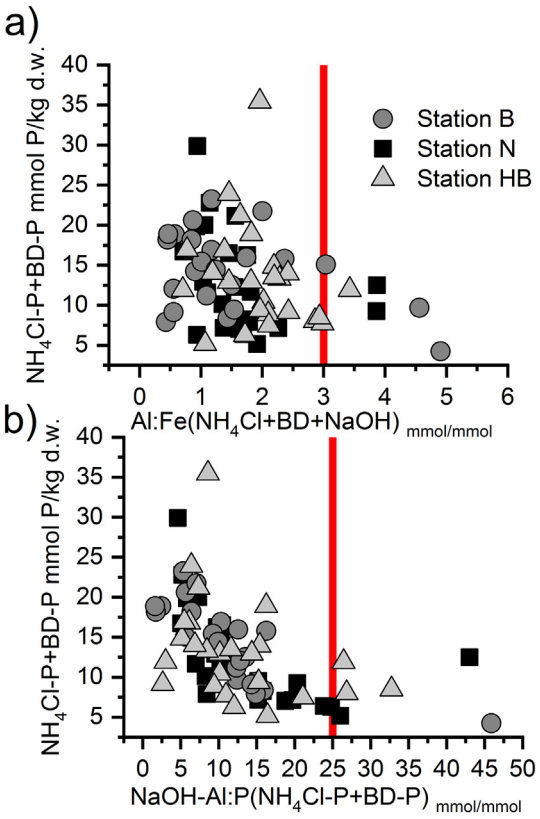

Fig. 13. (a) Molar ratios of Al vs. Fe against the sum of loosely sorbed (NH_4Cl) and redox-sensitive (BD-P) fractions, which are the most labile P forms. Kopáček's dataset ratio cut-off is indicated as a red line. (b) Sediment molar ratios of Al (associated with NaOH-SRP) vs. P[NH_4Cl + BD-P] against the sum of loosely sorbed (NH_4Cl) and redox-sensitive (BD-P) fractions. Kopáček's dataset ratio cut-off is indicated as a red line. Note that all ratios in (a) and (b) represent surface sediments (upper 5 cm). (For interpretation of the references to colour in this figure legend, the reader is referred to the web version of this article.)

Dittrich, 2013), which suggest that contrary to the traditional understanding of internal P loading, the oxygenation of lake bottom water is only one of several factors that control P release, which is triggered by both aerobic and anaerobic processes, in addition to sediment geochemical characteristics.

4.2. The importance of organic matter mineralization and iron reduction

Two main groups of processes promote P release from sediments: (1) the degradation of organic compounds, and (2) the desorption of P associated with various mineral compounds (e.g., aluminum hydroxides, clays, calcite) and reductive dissolution of redox sensitive compounds (e.g., iron oxyhydroxides) and subsequent release of associated P. To quantify the former, we calculated overall organic C degradation rates and compared them with short-term diffusive P fluxes. The ratios of estimated organic carbon degradation rates and short-term diffusive P fluxes are close to Redfield ratio, indicating that sediment P release is strongly related to decomposition of organic matter (Fig. 10a, b). Freshly deposited reactive organic matter has a C:P ratio that is generally assumed to be closed to 106:1, i.e., the Redfield ratio (Berner, 1977). While primarily representing stoichiometric nutrient relationships in marine phytoplankton, the Redfield ratio of fresh organic matter has been used in diverse aquatic settings including shallow wetlands, estuaries and deep lakes as an approximation of depositional flux of organic C and P (e.g., Ingall and Jahnke, 1997; Reed et al., 2011; Parsons et al., 2017; Li et al., 2018). Since the degradation of freshly deposited organic matter has significant impacts on regeneration of organic P, close agreement between diffusive P fluxes and estimated organic matter degradation rates indicates that short-term diffusive P release is most probably driven by the seasonal peak in organic debris accumulation, similar to other shallow eutrophic systems (e.g., Tammeorg et al., 2015; Parsons et al., 2017).

It is unlikely that all P liberated during organic matter mineralization will reach the overlying water. P release rates are often lower than predicted based on the organic matter mineralization rate (data below Redfield line, Fig. 10). This could suggest that P is trapped before being released from the sediment, either through scavenging by iron oxyhydroxides (e.g., Li et al., 2018) or as a result of authigenic mineral precipitation (e.g., vivianite, apatite) (Slomp et al., 1996; Rothe et al., 2015). Scavenged P represents labile pool vulnerable to microbial mediated reductive dissolution of iron oxyhydroxides. Redox potentials near sediment surface (< 5 cm depth, Fig. 2) are consistent with iron reduction conditions (Sigg, 2000; Tammeorg et al., 2015) and this shallow seated iron reduction zone leads to concurrent Fe and P release and correlation between fluxes of two elements, at stations B and N (Fig. 10). A similar correlation was not observed at station HB, however, despite low Eh values indicative of iron reduction in sediments close to the SWI (Fig. 2). Narrow range of Fe and P fluxes at this site (Fig. 5 and S3), indicates that system may be conducive to authigenic precipitation of Fe(II)-P phase (vivianite), which is commonly identified in organic rich lake sediments (e.g., Rothe et al., 2015). Indeed, calculated SRP and Fe^{2+} activities indicate that pore water was largely supersaturated with respect to vivianite (Fig. S6) throughout study period.

4.3. P diagenetic transformations

Diagenetic processes are reflected in transfers between P binding pools with sediment age which involved diagenetic remineralization of BD-P, NaOH-SRP and NaOH-NRP and concurrent precipitation of Ca-bound P with increasing sediment depth (Figs. 8, 9). While NaOH-SRP is often considered inert and strongly coupled with redox insensitive Al hydroxides (Kopáček et al., 2005), our results highlight the complex nature of this binding pool (Lukkari et al., 2007) at least partially composed of diagenetically reactive phases, which are remineralized with sediment depth and thus contribute to P recycling (Figs. 8, 9). Notwithstanding potential presence of reactive phases in this extraction pool, Al hydroxides are also moderately soluble at pH > 8 frequently observed in Bay of Quinte sediments (Boström et al., 1982; Cooke et al., 1993; pH range in Fig. 2), while their P binding capacity is reduced due to ligand exchange reactions in which hydroxide ions replace phosphate (Andersen, 1975; Lijklema 1976 & 1980). Furthermore, high Si concentrations in pore water likely promote competitive P desorption (Fig. 7), because Si is preferentially bound to Al-hydroxide sorption sites (Koski-Vähälä et al., 2001).

Concentrations of calcium-bound (HCl-P) increased with depth at stations N and HB (Fig. 8), indicating a diagenetic sink switching from labile forms (e.g., organic P and redox-sensitive P) to redox-stable HCl-P. External input due to erosion of Paleozoic carbonate bedrock in the watershed could represent one potential source of calcium-bound P. However this is unlikely the cause of its increase with sediment depth because in the time period covered by our sediment cores (Figs. 8, S4), there was no drastic change of population density and land use in the watersheds of these two stations. The spike in erosion linked to rapid deforestation in the area ended by the late 1800s (Schelske et al., 1985). On the other hand, it is possible that the applied extraction protocol overestimates HCl-P due to precipitation of Ca-P phases in previous NaOH step, as suggested by de Groot and Golterman (1990). The evaluation of extraction techniques by Hupfer et al. (2009), however, did not show appreciable overestimation of Ca-P phases in natural calcareous sediments with considerably higher carbonate content. This was related to the presence of humic acids and the addition of EDTA, which

form complexes with Ca and thus inhibit the precipitation of calcium phosphates (Hupfer et al., 2009). Thus, we suggest that an increase of Ca-bound P represents diagenetic immobilization (Ca-phosphate minerals precipitation, Dittrich and Koschel, 2002; Dittrich et al., 2011) (Fig. 9a; Fig. 11).

Ca-phosphate authigenesis is indicated by sharp increases of Ca concentrations in pore water compared to overlying lake water, reflecting either the dissolution of calcium carbonates or the desorption from humic acid complexes due to decreasing pH in sediment (Gerke and Hermann, 1992), or both. Furthermore, the presence of considerable amount of BD-P in deeper sediments (Fig. 8) undergoing continuous reductive dissolution is commonly understood to promote authigenic Ca-P formation (Slomp et al., 1996). As a result of elevated Ca and P concentrations, pore water is effectively supersaturated with respect to apatite near the SWI (Fig. 11). While we did not measure in situ pH in sediment deeper than 6 cm and thus cannot calculate saturation indices, we hypothesize that increasing Ca concentrations with depth (Fig. 7) along with higher P (Fig. 5) offset the likely pH decline.

4.4. Sediment P retention – role of Fe, Al and Ca

In lake sediments with sorption capacities dominated by iron oxyhydroxides, the ratio of Fe to P in sediment pore water is an indicator of the capacity of the sediment to maintain an oxidized surface iron layer as a barrier against P release (Smolders et al., 2001). If it is > 1–2, a sufficient amount of iron is available in the sediments, which promotes formation of the iron-coating layer at the SWI that suppresses internal P loading. In our study sites, this ratio was generally < 1 (Fig. S3), which suggests that the iron content in the sediments is not sufficient to prevent P internal loading.

BD-Fe:BD-P ratios of redox-sensitive P binding pools reflect the binding capacities of iron oxyhydroxides in sediment (Anschutz et al., 1998). For example, surface binding sites of nanoscale ferrihydrate, which is the phase with the highest binding capacity, are supersaturated when this ratio is around 6.7:1 (Sigg and Stumm, 1981). Higher ratios indicate spare binding capacity, provided that the sediment is composed solely of ferrihydrite, which is likely not the case, and other phases with fewer binding sites may also be present. At station N, BD-Fe:BD-P ratios were close to values indicating maximum sorption, while at stations B and HB these ratios were higher (11.2,1) and lower (6.4,1) than the theoretical maximum, respectively (Fig. 12). This suggests that sediments are close to saturation, with limited capacity to scavenge additional P.

In addition to reducible iron, sediment Al content is generally thought to contribute to permanent (diagenetically stable) P retention. Kopáček et al. (2005) showed that Al-rich sediments retain P due to sorption on aluminum hydroxide [$Al(OH)_3$], which is insensitive to redox changes. In the Bay of Quinte surface sediments, Al:Fe and Al:P ratios were generally lower than empirical cut-offs based on the Kopáček et al. (2005) dataset (< 3 and < 25, for Al:Fe and Al:P, respectively, Fig. 13) suggesting that reductive dissolution of Fe (III) oxyhydroxides carries a risk of internal P loading, while sediment content of the redox-insensitive $Al(OH)_3$ is too small to inhibit the release of P. While sink switching in surface sediment is ineffective to prevent P release, relatively high pH in the Bay of Quinte sediment limits the effectiveness of P sorption on $Al(OH)_3$ and may lead to the dissolution of some $Al(OH)_3$, which is reflected in decreasing NaOH-SRP concentrations with depth (see Fig. 8) and generally poor coupling between P and Al (Section 4.3; Tables S4–S6).

In contrast to the lakes included in Kopáček et al. (2005) study, the retention capacity of the Bay of Quinte sediments is maintained by sink switching to HCl-P (Fig. 9) likely representing authigenesis of apatite due to its supersaturation in pore water (Fig. 11). However, the magnitude of P immobilization in HCl-P is < 15% of the long-term mobilization of labile P forms (Fig. 9).

4.5. The magnitude of long-term P release and implications

Extrapolating the average long-term release rates across the entire area of the three basins (80 km^2, 18 km^2 and 22.5 km^2 for the Belleville, Napanee and Hay Bay basins, respectively, Kim et al., 2013), we estimate fluxes of 120 kg P/day, 25 kg P/day and 44 kg P/day for the Belleville, Napanee and Hay Bay basins, respectively. These results are on par with the P mass balance model delineations by Kim et al. (2013) and Arhonditsis et al. (2016). For comparison, the sum of external P inputs and transfers downstream from the upper reaches of the Bay of Quinte are 206 kg P/day and 226 kg P/day for the Belleville and Napanee basins (Arhonditsis et al., 2016). This magnitude of sediment P release, in combination with low retention, has important implications for loading control, because rapid sediment P recycling tends to retain P in the lake basin. In shallow lakes, sediment P release is amplified by fast particle settling, which increases deposition of diagentically reactive P phases in sediments and thus promotes subsequent internal loading (Katsev, 2017). External P loading reduction elicits rapid lake response if the hydrological residence time is short (Katsev, 2017), but in systems with high sediment P recycling rates this quickly results in the dominance of sediments as the nutrient source. The Bay of Quinte eutrophication history demonstrates such behavior. In the early days of P control, a large P loading reduction achieved an immediate, significant decrease of the ambient P level, while the subsequent input reductions were smaller and obeying the law of diminishing returns have largely stabilized water column P levels in the past couple of decades. Currently, P levels are largely maintained through intensive P recycling in the sediment, contributing as much as 50% of the overall external P inputs in the uppermost Belleville basin.

This study of the Bay of Quinte underscores the important role of sediment P diagenesis in lake nutrient budgets and emphasizes the need for investigations of sediment internal loading in lakes undergoing nutrient management. Multiple approaches, including in situ measurements and sediment P fractions, are required to cover different areas of the lake and to capture seasonal variability over multiple years in order to quantify this important flux (Matisoff et al., 2016; Orihel et al., 2017). Furthermore, as sediment P recycling is ultimately fueled by particle settling, which removes P from the water, sedimentation rates obtained using sediment trap measurements or radioisotope dating, or both, should constrain this P transfer.

5. Conclusions

In this study, we investigated processes that control sediment P dynamics in a shallow hard water eutrophic lake experiencing drastically reduced external P inputs. We observed that despite well-oxygenated bottom waters throughout most of the study period, short-term diffusive P fluxes were considerable at all studied stations. Importantly, our data show that significant P-flux occurs in shallow areas, with an apparent discordance with concurrent measures of long-term P release from the sediments. Not only do these results challenge the paradigm describing sediment P release from shallow systems, but they also demonstrate that short-term measures cannot be extrapolated to long-term estimates (and vice versa).

The mobilization of organic P moderated by sorption/desorption processes coupled with redox-sensitive Fe cycling was found to be the main contributor to internal P loading, while P immobilization was driven by the precipitation of apatite (Fig. 11). Sediment P sorption capacity was not enhanced by Al, due to the moderately alkaline pH conditions reflective of carbonate bedrock in the watershed and elevated Si concentrations in pore water, which promote competitive P desorption. Sediment retention of deposited P was fairly low (~60% of the total P) and even lower for labile P forms (35%–40%), indicative of intensive diagenetic P recycling.

This intensive sediment P recycling has considerable implications for the management of eutrophication in the Bay of Quinte, since this

flux cannot easily be moderated. While any intervention to reduce P release in the whole basin is likely prohibitive due to lake size, limited-scope intervention to enhance existing processes of P sequestration in hot spots may be cost effective (e.g., by adding $Ca(OH)_2$ to promote the ongoing precipitation of Ca-P phases, Dittrich et al., 2011). Sediment P release appears to be driven largely by the degradation of recently deposited organic matter coupled with desorption of Fe-bound P, implying that sediments will continue to be a major source for the extended period of time. Surface sediments have a limited capacity to bind any newly deposited P, which underscores the importance of continuing efforts to control point and non-point sources of P in the Bay of Quinte watershed.

Our findings suggest that internal P loading displays pronounced temporal and spatial variability, which is at least partially driven by organic matter flux to sediment, mineralogical and geochemical characteristics of freshly deposited sediment. This emphasizes the importance of the characterization of riverine P supply, i.e., the chemical and mineralogical composition, and the mode and timing of sediment delivery, particularly in lakes that experience persistent eutrophication despite the reduction of point source inputs.

Acknowledgements

Funding by the Great Lakes Sustainability Fund, Canada (GCXE17P158), Environment and Climate Change Canada, Ministry of the Environment and Climate Change and Lower Trent Conservation Authority, Bay of Quinte Remediation Action plan Office to MD is greatly acknowledged. We also thank the Environment and Climate Change Canada and Quinte Conservation technical operations personnel for invaluable assistance in the field. Furthermore, field and lab assistance by Oleksandra Kaskun, Elaine Lu, Preksha Surana and Yijing Cui is greatly acknowledged.

Appendix A. Supplementary data

Supplementary data to this article can be found online at https://doi.org/10.1016/j.chemgeo.2019.03.031.

References

Aller, R.C., 1994. Bioturbation and remineralization of sedimentary organic matter: effects of redox oscillation. Chem. Geol. 114, 331–345. https://doi.org/10.1016/0009-2541(94)90062-0.

Andersen, J.M., 1975. Influence of pH on release of phosphorus from lake sediments. Arch. für Hydrobiol. 76, 411–419.

Anschutz, P., Zhong, S., Sundby, B., Mucci, A., Gobeil, C., 1998. Burial efficiency of phosphorus and the geochemistry of iron in continental margin sediments. Limnol. Oceanogr. 43, 53–64. https://doi.org/10.4319/lo.1998.43.1.0053.

Appleby, P.G., Oldfield, F., 1978. The calculation of lead-210 dates assuming a constant rate of supply of unsupported 210Pb to the sediment. Catena 5, 1–8. https://doi.org/10.1016/S0341-8162(78)80002-2.

Arhonditsis, G. B., D. K. Kim, Y. Shimoda, and others. 2016. Integration of best management practices in the Bay of Quinte watershed with the phosphorus dynamics in the receiving waterbody: what do the models predict? Aquat. Ecosyst. Heal. Manag. 19: 1–18. doi:https://doi.org/10.1080/14634988.2016.1130566.

Armstrong, D.K., Dodge, J.E.P., 2007. Paleozoic geology of southern Ontario. Ontario Geol. Surv. Miscellaneous Release-Data 219.

Bailey, R.C., Grapentine, L., Stewart, T.J., Schaner, T., Chase, M.E., Mitchell, J.S., Coulas, R.A., 1999. Dreissenidae in Lake Ontario: Impact assessment at the whole lake and Bay of Quinte spatial scales. J. Great Lakes Res. 25, 482–491. https://doi.org/10.1016/S0380-1330(99)70756-2.

Berner, R.A., 1977. Stoichiometric models for nutrient regeneration in anoxic sediments. Limnol. Oceanogr. 22, 781–786. https://doi.org/10.4319/lo.1977.22.5.0781.

Berner, R.A., 1980. Early Diagenesis: a Theoretical Approach, Princeton Series in Geochemistry. Princeton University Press, Princeton, N.J.

Boström, B., Jansson, M., Forsberg, C., 1982. Phosphorus release from lake sediments. Arch. für Hydrobiol. Beih. Ergebn Limnol. 18, 5–59.

Boudreau, B.P., 1997. Diagenetic models and their implementation. Modelling transport and reactions in aquatic sediments, Springer, New York. doi:0.I007/97S-3-642-60421-S.

Burdige, D.J., 2006. Geochemistry of Marine Sediments. Princeton University Presshttps://doi.org/10.1086/533614.

Carey, C.C., Rydin, E., 2011. Lake trophic status can be determined by the depth distribution of sediment phosphorus. Limnol. Oceanogr. 56, 2051–2063. https://doi.org/10.4319/lo.2011.56.6.2051.

Cooke, G.D., Welch, E.B., Martin, A.B., Fulmer, D.G., Hyde, J.B., Schrieve, G.D., 1993. Effectiveness of Al, Ca, and Fe salts for control of internal phosphorus loading in shallow and deep lakes. Hydrobiologia 253, 323–335. https://doi.org/10.1007/BF00050758.

Currie, W.J.S., and M.M. Frank. 2015. Multivariate analysis of the 40 year Project Quinte biogeochemistry dataset: water chemistry, physical characteristics, seston and climate. Can. Tech. Rep. Fish. Aquat. Sci. 3125: vi: + 65p.

de Groot, C.J., Golterman, H.L., 1990. Sequential fractionation of sediment phosphate. Hydrobiologia 192, 143–148. https://doi.org/10.1007/BF00006010.

Depew, D.C., Koehler, G., Hiriart-Baer, V., 2018. Phosphorus dynamics and availability in the nearshore of Eastern Lake Erie: insights from oxygen isotope ratios of phosphate. Front. Mar. Sci. 5. https://doi.org/10.3389/fmars.2018.00215.

Dittrich, M., Koschel, R., 2002. Interactions between calcite precipitation (natural and artificial) and phosphorus cycle in the hardwater lake. Hydrobiologia 469, 49–57. https://doi.org/10.1023/A:1015571410442.

Dittrich, M., Gabriel, O., Rutzen, C., Koschel, R., 2011. Lake restoration by hypolimnetic Ca(OH)2 treatment: Impact on phosphorus sedimentation and release from sediment. Sci. Total Environ. 409, 1504–1515. https://doi.org/10.1016/j.scitotenv.2011.01.006.

Dittrich, M., A. Chesnyuk, A. Gudimov, and others. 2013. Phosphorus retention in a mesotrophic lake under transient loading conditions: insights from a sediment phosphorus binding form study. Water Res. 47: 1433–1447. doi:https://doi.org/10.1016/j.watres.2012.12.006.

Gerke, J., Hermann, R., 1992. Adsorption of orthophosphate to humic-Fe-complexes and to amorphous Fe-oxide. Z. Pflanzenernähr. Bodenkd. 155, 233–236. https://doi.org/10.1002/jpln.19921550313.

Geurts, J.J.M., Smolders, A.J.P., Verhoeven, J.T.A., Roelofs, J.G.M., Lamers, L.P.M., 2008. Sediment Fe:PO4 ratio as a diagnostic and prognostic tool for the restoration of macrophyte biodiversity in fen waters. Freshw. Biol. 53, 2101–2116. https://doi.org/10.1111/j.1365-2427.2008.02038.x.

Hecky, R.E., Smith, R.E., Barton, D.R., Guildford, S.J., Taylor, W.D., Charlton, M.N., Howell, T., 2004. The nearshore phosphorus shunt: a consequence of ecosystem engineering by dreissenids in the Laurentian Great Lakes. Can. J. Fish. Aquat. Sci. 61, 1285–1293. https://doi.org/10.1139/f04-065.

Howell, T., Marvin, C.H., Bilyea, R.W., Kauss, P.B., Somers, K., 1996. Changes in environmental conditions during Dreissena colonization of a monitoring station in Eastern Lake Erie. J. Great Lakes Res. 22, 744–756. https://doi.org/10.1016/S0380-1330(96)70993-0.

Hupfer, M., Lewandowski, J., 2005. Retention and early diagenetic transformation of phosphorus in Lake Arendsee (Germany) – consequences for management strategies. Arch. für Hydrobiol. 164, 143–167. https://doi.org/10.1127/0003-9136/2005/0164-0143.

Hupfer, M., Lewandowski, J., 2008. Oxygen controls the phosphorus release from lake sediments - a long-lasting paradigm in limnology. Int. Rev. Hydrobiol. 93, 415–432. https://doi.org/10.1002/iroh.200711054.

Hupfer, M., Gächter, R., Giovanoli, R., 1995. Transformation of phosphorus species in settling seston and during early sediment diagenesis. Aquat. Sci. 57, 305–324. https://doi.org/10.1007/BF00878395.

Hupfer, M., Rübe, B., Schmieder, P., 2004. Origin and diagenesis of polyphosphate in lake sediments: A31P-NMR study. Limnol. Oceanogr. 49, 1–10. https://doi.org/10.4319/lo.2004.49.1.0001.

Hupfer, M., Zak, D., Roßberg, R., Herzog, C., Pöthig, R., 2009. Evaluation of a well-established sequential phosphorus fractionation technique for use in calcite-rich lake sediments: identification and prevention of artifacts due to apatite formation. Limnol. Oceanogr. Methods 7, 399–410. https://doi.org/10.4319/lom.2009.7.399.

Ingall, E., Jahnke, R., 1994. Evidence for enhanced phosphorus regeneration from marine sediments overlain by oxygen depleted waters. Geochim. Cosmochim. Acta 58, 2571–2575. https://doi.org/10.1016/0016-7037(94)90033-7.

Ingall, E., Jahnke, R., 1997. Influence of water-column anoxia on the elemental fractionation of carbon and phosphorus during sediment diagenesis. Mar. Geol. https://doi.org/10.1016/S0025-3227(96)00112-0.

Jensen, H.S., Andersen, F.O., 1992. Importance of temperature, nitrate, and pH for phosphate release from aerobic sediments of four shallow, eutrophic lakes. Limnol. Oceanogr. 37, 577–589. https://doi.org/10.4319/lo.1992.37.3.0577.

Jørgensen, B.B., 1982. Mineralization of organic matter in the sea bed - the role of sulphate reduction. Nature 296, 643–645. https://doi.org/10.1038/296643a0.

Katsev, S., 2017. When large lakes respond fast: a parsimonious model for phosphorus dynamics. J. Great Lakes Res. 43, 199–204. https://doi.org/10.1016/j.jglr.2016.10.012.

Katsev, S., Dittrich, M., 2013. Modeling of decadal scale phosphorus retention in lake sediment under varying redox conditions. Ecol. Model. 251, 246–259. https://doi.org/10.1016/j.ecolmodel.2012.12.008.

Katsev, S., Tsandev, I., L'Heureux, I., Rancourt, D.G., 2006. Factors controlling long-term phosphorus efflux from lake sediments: Exploratory reactive-transport modeling. Chem. Geol. 234, 127–147. https://doi.org/10.1016/j.chemgeo.2006.05.001.

Kim, D. K., W. Zhang, Y. R. Rao, and others. 2013. Improving the representation of internal nutrient recycling with phosphorus mass balance models: a case study in the Bay of Quinte, Ontario, Canada. Ecol. Modell. 256: 53–68. doi:https://doi.org/10.1016/j.ecolmodel.2013.02.017.

Kopáček, J., Borovec, J., Hejzlar, J., Ulrich, K.U., Norton, S.A., Amirbahman, A., 2005. Aluminum control of phosphorus sorption by lake sediments. Environ. Sci. Technol. 39, 8784–8789. https://doi.org/10.1021/es050916b.

Koski-Vähälä, J., Hartikainen, H., Tallberg, P., 2001. Phosphorus mobilization from various sediment pools in response to increased pH and silicate concentration. J.

Environ. Qual. 30, 546. https://doi.org/10.2134/jeq2001.302546x.
Laskov, C., Herzog, C., Lewandowski, J., Hupfer, M., 2007. Miniaturized photometrical methods for the rapid analysis of phosphate, ammonium, ferrous iron, and sulfate in pore water of freshwater sediments. Limnol. Oceanogr. Methods 5, 63–71. https://doi.org/10.4319/lom.2007.5.63.
Lewandowski, J., Hupfer, M., 2005. Effect of macrozoobenthos on two-dimensional small-scale heterogeneity of pore water phosphorus concentrations in lake sediments: a laboratory study. Limnol. Oceanogr. 50, 1106–1118. https://doi.org/10.4319/lo.2005.50.4.1106.
Lewandowski, J., Rüter, K., Hupfer, M., 2002. Two-dimensional small-scale variability of pore water phosphate in freshwater lakes: results from a novel dialysis sampler. Environ. Sci. Technol. 36, 2039–2047. https://doi.org/10.1021/es0102538.
Lewandowski, J., Laskov, C., Hupfer, M., 2007. The relationship between Chironomus plumosus burrows and the spatial distribution of pore-water phosphate, iron and ammonium in lake sediments. Freshw. Biol. https://doi.org/10.1111/j.1365-2427.2006.01702.x.
Li, J., Crowe, S.A., Miklesh, D., Kistner, M., Canfield, D.E., Katsev, S., 2012. Carbon mineralization and oxygen dynamics in sediments with deep oxygen penetration, Lake Superior. Limnol. Oceanogr. 57, 1634–1650. https://doi.org/10.4319/lo.2012.57.6.1634.
Li, J., Zhang, Y., Katsev, S., 2018. Phosphorus recycling in deeply oxygenated sediments in Lake Superior controlled by organic matter mineralization. Limnol. Oceanogr. 63, 1372–1385. https://doi.org/10.1002/lno.10778.
Lijklema, L., 1976. The role of iron in the exchange of phosphate between water and sediments. Interactions Between Sediments and Fresh Water: Proceedings of an International Symposium Held at Amsterdam, the Netherlands. September 6–10 (1976), 313–317.
Lijklema, L., 1980. Interaction of Orthophosphate With Iron(III) and Aluminum Hydroxides. Environ. Sci. Technol. 14, 537–541. https://doi.org/10.1021/es60165a013.
Lukkari, K., Hartikainen, H., Leivuori, M., 2007. Fractionation of sediment phosphorus revisited. I: Fractionation steps and their biogeochemical basis. Limnol. Oceanogr. Methods 5, 433–444. https://doi.org/10.4319/lom.2007.5.433.
Maerki, M., Müller, B., Dinkel, C., Wehrli, B., 2009. Mineralization pathways in lake sediments with different oxygen and organic carbon supply. Limnol. Oceanogr. 54, 428–438. https://doi.org/10.4319/lo.2009.54.2.0428.
Malmaeus, J., Rydin, E., Jonsson, P., Lindgren, D., Magnus Karlsson, O., 2012. Estimating the amount of mobile phosphorus in baltic coastal soft sediments of central Sweden. Boreal Environ. Res. 17, 425–436.
Manning, P.G., 1996. Bioavailability of riverine, sewage plant, and sediment phosphorus in the Bay of Quinte, Lake Ontario. Can. Mineral. 34, 667–675.
Mathieu, G., Biscayne, P., Lupton, R., Hammond, D., 1988. System for measurements of 222Rn at low levels in natural waters. Health Phys. 55, 989–992.
Matisoff, G., Lou Carson, M., 2014. Sediment resuspension in the Lake Erie nearshore. J. Great Lakes Res. 40, 532–540. https://doi.org/10.1016/j.jglr.2014.02.001.
Matisoff, G., Kaltenberg, E.M., Steely, R.L., Hummel, S.K., Seo, J., Gibbons, K.J., Bridgeman, T.B., Seo, Y., Behbahani, M., James, W.F., Johnson, L.T., Doan, P., Dittrich, M., Evans, M.A., Chaffin, J.D., 2016. Internal loading of phosphorus in western Lake Erie. J. Great Lakes Res. 42, 775–788. https://doi.org/10.1016/j.jglr.2016.04.004.
Minns, C.K., Owen, G.E., Johnson, M.G., 1986. Nutrient loads and budgets in the Bay of Quinte, Ontario, p.50-58. In C. K. Minns, D. A. Hurley, and K. H. Nicholls [eds.] Project Quinte: Point-source Phosphorus Control land Ecosystem Response in the Bay of Quinte, Lake Ontario. Can. Spec. Pub I. Fish. Aquat. Sci. In: 86.
Minns, C.K., Moore, J.E., Doka, S.E., John, M.A.St., 2011. Temporal trends and spatial patterns in the temperature and oxygen regimes in the Bay of Quinte, Lake Ontario, 1972–2008. Aquat. Ecosyst. Heal. Manag. 14, 9–20. https://doi.org/10.1080/14634988.2011.547327.
Mortimer, C.H., 1942. The exchange of dissolved substances between mud and water in lakes. J. Ecol. 30, 147. https://doi.org/10.2307/2256691.
Mosley, C., Bootsma, H., 2015. Phosphorus recycling by profunda quagga mussels (Dreissena rostriformis bugensis) in Lake Michigan. J. Great Lakes Res. https://doi.org/10.1016/j.jglr.2015.07.007.
Nicholls, K.H., Hoyle, J.A., Johannsson, O.E., Dermott, R., 2011. A biological regime shift in the Bay of Quinte ecosystem (Lake Ontario) associated with the establishment of invasive dreissenid mussels. J. Great Lakes Res. 37, 310–317. https://doi.org/10.1016/j.jglr.2010.12.004.
Norton, S.A., Coolidge, K., Amirbahman, A., Bouchard, R., Kopáček, J., Reinhardt, R., 2008. Speciation of Al, Fe, and P in recent sediment from three lakes in Maine, USA. Sci. Total Environ. 404, 276–283. https://doi.org/10.1016/j.scitotenv.2008.03.016.
Orihel, D.M., Baulch, H.M., Casson, N.J., North, R.L., Parsons, C.T., Seckar, D.C.M., Venkiteswaran, J.J., 2017. Internal phosphorus loading in Canadian fresh waters: a critical review and data analysis. Can. J. Fish. Aquat. Sci. 1–25. https://doi.org/10.1139/cjfas-2016-0500.
Ozersky, T., Barton, D.R., Hecky, R.E., Guildford, S.J., 2013. Dreissenid mussels enhance nutrient efflux, periphyton quantity and production in the shallow littoral zone of a large lake. Biol. Invasions 15, 2799–2810. https://doi.org/10.1007/s10530-013-0494-z.
Paraskova, J.V., Sjöberg, P.J.R., Rydin, E., 2014. Turnover of DNA-P and phospholipid-P in lake sediments. Biogeochemistry. https://doi.org/10.1007/s10533-014-9972-3.
Parkhurst, D. L., and C. A. J. Appelo. 2013. PHREEQC (Version 3)-A Computer Program for Speciation, Batch-Reaction, One-Dimensional Transport, and Inverse Geochemical Calculations. Model. Tech. B. 6 497. doi:Rep. 99–4259.
Parsons, C.T., Rezanezhad, F., O'Connell, D.W., Van Cappellen, P., 2017. Sediment phosphorus speciation and mobility under dynamic redox conditions. Biogeosciences 14, 3585–3602. https://doi.org/10.5194/bg-14-3585-2017.
Psenner, R., Pucsko, R., 1988. Phosphorus fractionation: Advantages and limits of the method for the study of sediment P origins and interactions. Arch. Hydrobiol. Beih. Ergeb. Limnol. 30, 43–59.
Puttonen, I., Mattila, J., Jonsson, P., Karlsson, O.M., Kohonen, T., Kotilainen, A., Lukkari, K., Malmaeus, J.M., Rydin, E., 2014. Distribution and estimated release of sediment phosphorus in the northern Baltic Sea archipelagos. Estuar. Coast. Shelf Sci. 145, 9–21. https://doi.org/10.1016/j.ecss.2014.04.010.
Redfield, A.C., B.H. Ketchum, and F.W. Richards. 1963. The influence of organisms on the composition of sea water p. 26–77. In: Hill, M.N. [ed], The sea, 2, Wiley Interscience, NY.
Reed, D.C., Slomp, C.P., Gustafsson, B.G., 2011. Sedimentary phosphorus dynamics and the evolution of bottom-water hypoxia: a coupled benthic-pelagic model of a coastal system. Limnol. Oceanogr. 56, 1075–1092. https://doi.org/10.4319/lo.2011.56.3.1075.
Rothe, M., Kleeberg, A., Grüneberg, B., Friese, K., Pérez-Mayo, M., Hupfer, M., 2015. Sedimentary Sulphur:iron ratio indicates vivianite occurrence: a study from two contrasting freshwater systems. PLoS One 10. https://doi.org/10.1371/journal.pone.0143737.
Rydin, E., 2000. Potentially mobile phosphorus in Lake Erken sediment. Water Res. 34, 2037–2042. https://doi.org/10.1016/S0043-1354(99)00375-9.
Rydin, E., Malmaeus, J.M., Karlsson, O.M., Jonsson, P., 2011. Phosphorus release from coastal Baltic Sea sediments as estimated from sediment profiles. Estuar. Coast. Shelf Sci. 92, 111–117. https://doi.org/10.1016/j.ecss.2010.12.020.
Schelske, C.L., D.J. Conley, and W.F. Warwick. 1985. Historical relationships between phosphorus loading and biogenic silica accumulation in Bay of Quinte sediments. Can. J. Fish. Aquat. Sci. 42: 1401–1489.
Shimoda, Y., Watson, S.B., Palmer, M.E., Koops, M.A., Mugalingam, S., Morley, A., Arhonditsis, G.B., 2016. Delineation of the role of nutrient variability and dreissenids (Mollusca, Bivalvia) on phytoplankton dynamics in the Bay of Quinte, Ontario, Canada. Harmful Algae 55, 121–136. https://doi.org/10.1016/j.hal.2016.02.005.
Shore, J.A., Valipour, R., Blukcacz-Richards, E.A., 2016. Twenty-eight years of hydrodynamic variability in the Bay of Quinte (ice-free periods of 1979–2006). J. Great Lakes Res. 42, 985–996. https://doi.org/10.1016/j.jglr.2016.07.005.
Sigg, L., 2000. Redox potential measurements in natural waters: significance, concepts and problems. In: Redox: Fundamentals, Processes, and Applications, pp. 1–12.
Sigg, L., Stumm, W., 1981. The interaction of anions and weak acids with the hydrous goethite (α-FeOOH) surface. Colloids and Surfaces 2, 101–117. https://doi.org/10.1016/0166-6622(81)80001-7.
Slomp, C.P., Epping, E.H.G., Helder, W., Van Raaphorst, W., 1996. A key role for iron bound phosphorus in authigenic apatite formation in North Atlantic continental platform sediments. J. Mar. Res. 54, 1179–1205.
Sly, P.G., 1986. Review of postglacial environmental changes and cultural impacts in the Bay of Quinte, p. 7-26. In C. K. Minns, D. A. Hurley, and K. H. Nicholls [eds.] Project Quinte: Point-source Phosphorus Control Land Ecosystem Response in the Bay of Quinte, Lake Ontario. Can. Spec. Pub I. Fish. Aquat. Sci. In: 86.
Sly, P.G., 1990. Experimental use of dialysis chamber arrays to study P-fluxes in the Bay of Quinte, 1987. J. Great Lakes Res. 16, 258–270. https://doi.org/10.1016/S0380-1330(90)71419-0.
Smith, V.H., Schindler, D.W., 2009. Eutrophication science: where do we go from here? Trends Ecol. Evol. 24, 201–207. https://doi.org/10.1016/j.tree.2008.11.009.
Smith, L., Watzin, M.C., Druschel, G., 2011. Relating sediment phosphorus mobility to seasonal and diel redox fluctuations at the sediment-water interface in a eutrophic freshwater lake. Limnol. Oceanogr. 56, 2251–2264. https://doi.org/10.4319/lo.2011.56.6.2251.
Smolders, A.J.P., Lamers, L.P.M., Moonen, M., Zwaga, K., Roelofs, J.G.M., 2001. Controlling phosphate release from phosphate-enriched sediments by adding various iron compounds. Biogeochemistry 54, 219–228. https://doi.org/10.1023/A:1010660401527.
Søndergaard, M., Jensen, J.P., Jeppesen, E., 2003. Role of sediment and internal loading of phosphorus in shallow lakes. Hydrobiologia 135–145.
Stoermer, E.F., Wolin, J.A., Schelske, C.L., 5 I Conley, E.F. Stoermer, Wolin, I.A., Conley, D.I., 1985. Postsettlement diatom succession in the Bay of Quinte, Lake Ontario. Can. J. Fish. Aquat. Sci. 42, 754–767. https://doi.org/10.1139/f85-097.
Tammeorg, O., Horppila, J., Laugaste, R., Haldna, M., Niemistö, J., 2015. Importance of diffusion and resuspension for phosphorus cycling during the growing season in large, shallow Lake Peipsi. Hydrobiologia 760, 133–144. https://doi.org/10.1007/s10750-015-2319-9.
Tammeorg, O., Horppila, J., Tammeorg, P., Haldna, M., Niemistö, J., 2016. Internal phosphorus loading across a cascade of three eutrophic basins: a synthesis of short- and long-term studies. Sci. Total Environ. 572, 943–954. https://doi.org/10.1016/j.scitotenv.2016.07.224.
Thibault, P.J., Rancourt, D.G., Evans, R.J., Dutrizac, J.E., 2009. Mineralogical confirmation of a near-P:Fe = 1:2 limiting stoichiometric ratio in colloidal P-bearing ferrihydrite-like hydrous ferric oxide. Geochim. Cosmochim. Acta 73, 364–376. https://doi.org/10.1016/j.gca.2008.10.031.
USEPA, 1982. Handbook for Sampling and Sample Preservation of Water and Wastewater. In: EPA-600/4-82-029. United States Environmental Protection Agency, Cincinnati, OH.
Warwick, W.F., 1980. Paleolimnology of the Bay of Quinte, Lake Ontario: 2800 years of cultural influence. Can. Bull. Fish. Aquat. Sci. 206 (117 p.).
Wilson, T.A., Amirbahman, A., Norton, S.A., Voytek, M.A., 2010. A record of phosphorus dynamics in oligotrophic lake sediment. J. Paleolimnol. 44, 279–294. https://doi.org/10.1007/s10933-009-9403-y.

Supplementary online material

Table S1: Sampling dates (2013-2016)

Date (day.month)										
Year	2013	2014				2015			2016	
Core sampling	13.8	25.2	21.5	21.7	20.10.	28.5	18.8	28.9	2.8	12.9
Peeper deployment	N/A	24.2-11.3	20.5-4.6	21.7-5.8	20.10-4.11	28.5-9.6	11.8-26-8	28.9-7.10	27.7-11.8	6-22.09

1 Microsensor calibration and measurements

Oxygen concentrations were measured using a Clark-type O_2 microelectrode (Unisense OX50, Denmark). The electrode was calibrated with air-saturated deionized water (1 hour vigorous air bubbling in the Unisense calibration chamber) and zero reading obtained with O_2-free sodium hydrosulfite solution. The pH electrodes (Unisense pH-N, Denmark) were calibrated with commercial pH buffers (pH 4, 7 and 9, HACH). The redox potential (reduction potential measured in mV) was measured with a Unisense redox electrode relative to Radiometer Analytical reference electrode. The offset between the reference electrode and standard hydrogen electrode potential was calibrated prior to measurement using freshly prepared quinhydrone redox buffers with defined redox potentials.

The pore water $H_2S_{(g)}$ was measured using a Unisense amperometric ferricyanide microsensor sensor. Since ferricyanide electrolyte is sensitive to light, it was calibrated in a darkened calibration chamber and all measurements were conducted in the dark. A three-point calibration in the range 0 to 100 μmol H_2S was conducted using oxygen-free standards prepared from 10 mM Na_2S stock solution. The sum of all sulfide species (total sulfide) was calculated from measured pH and $H_2S_{(g)}$ using the theoretically predicted equilibrium relationship described in Jeroschewski et al. (1996).

Table S2. Organic carbon and nitrogen in surface sediments (0-1 cm)

Station/Date	August 2014		C:N [mol:mol]	October 2014		C:N [mol:mol]
	Organic C [mg/g d.w]	Organic N [mg/g d.w]		Organic C [mg/g d.w]	Organic N [mg/g d.w]	
B	116.5	15.85	8.6	118.5	17.2	8.0
N	112.3	15.39	8.5	110.2	16.43	7.8
HB	106	15.14	9.5	103	15.57	9.5

Table S3. Calculated diffusive fluxes of Mn^{2+}, Ca^{2+}, Si, SO^{2+}_4, NH_4^+

Diffusive flux	**Sampling date**	**Station B**	**Station N**	**Station HB**
		mg/m^2/day	mg/m^2/day	mg/m^2/day
Mn	August 2014	9.110179	8.34602	1.87101
	August 2015	7.68563	3.16521	1.94687
	September 2015	3.09724	1.22607	1.75151
Ca	August 2014	35.3822	63.43034	17.5023
	August 2015	55.47033	21.1578	12.01205
	September 2015	42.03239	11.52495	20.10117
Si	August 2014	86.52034	49.31821	42.68587
	August 2015	32.13593	25.56852	11.82812
	September 2015	18.36506	13.97167	11.91806
SO_4^{2-}	August 2016	54.4715	42.64148	85.14228
	September 2016	28.32361	46.77082	57.4389
NH_4^+	August 2016	22.06332	15.00147	14.27879
	September 2016	8.14436	10.57621	14.17098

2 Organic carbon mineralization rates

Sediment oxygen consumption reflects aerobic organic matter mineralization as well as oxidation of reduced compounds (Fe^{2+}, Mn^{2+}, NH_4^+) produced by anaerobic organic matter degradation processes. The contribution of Mn and Fe reduction appears to be minor, constituting up to ~1%-2% of the total organic matter degradation (Table 1 in the main text; Table S3). A slightly higher amount of organic C was remineralized through sulfate reduction (5%-10% of total degradation rates), leaving the fermentation processes (e.g., methanogenesis) as the main organic matter mineralization pathway in the Bay of Quinte sediments (Table 1 in main text; Table S3). Furthermore, since our estimate did not account for *in situ* precipitation of iron sulfides, the contribution of iron and sulfate reduction is likely higher. Manning (1996) showed that the total sulfur concentration in the Bay of Quinte sediments is ~ 0.5 % dry weight. If we assume that this represents the upper limit of iron sulfide concentration, we can estimate the maximum rate of sulfide precipitation using our sediment accumulation rates. This amounts to iron sulfide precipitation of 0.21 mmol S/m^2/d, 0.385 mmol S/m^2/d and 0.385 mmol S/m^2/d for stations B, N and HB, respectively. Since for every mol of S^{2-} produced two mol of C are oxidized, the organic matter degradation rates not accounted in our estimates are 0.42, 0.77 and 0.77 mmol C/m^2/d (station B, N and HB respectively), considerably less than total estimated organic matter degradation rates at these sites (5-10% of total). On the other hand, these sulfide precipitation rates are close to our sulfate reduction rates calculated from sulfate diffusive gradients, which suggests that a large portion of sulfide is quickly sequestered in iron sulfides and helps explain the absence of pore water accumulation of H_2S concurrently with sulfate depletion, as suggested by our microsensor measurements.

NH_4^+ diffusive fluxes (Table S3) calculated from the concentration gradients (Figure 7 in the main text) present a minimum estimate of the rate of anaerobic organic matter mineralization (Maerki et al 2009). With the assumption that organic C and organic N are released at the constant ratio equal to C:N ratio in surface sediments (Table S2), we estimated the overall anaerobic organic matter degradation. The anaerobic processes dominate the organic matter decomposition, and their relative contribution increased with water depth, from the shallowest station B to the deepest station HB. The actual rates of anaerobic processes could have been greater, due to the oxidation of NH_4^+ to NO_3^- in the uppermost sample. Bottom lake water and pore water NO_3^- concentrations

at all stations during this period, however, were <1μmol/l, while oxygen penetration depths were extremely shallow (1-2 mm), suggesting that NH_4^+ oxidation below SWI was negligible.

3 Pearson's correlation coefficients between metals and P in key binding pools

In order to gain insights into the mineral associations comprising P binding pools and their diagenetic transformations, we calculated Pearson's correlation coefficients between P and mobilized metals in key fractions contributing to burial and release (Tables S4-S6). Immediately apparent were the very strong positive correlations between BD-Fe and BD-P (Pearson's r=0.68 at station B, 0.82 and 0.87 at N and HB respectively) and moderate to very strong correlation between BD-Mn and BD-P (r=0.47 at station B) and (r=0.82 at station N; r=0.93 at HB). Statistically significant, albeit moderate, correlations were found between acid-soluble HCl-P and HCl-Ca extracted in Step 4. Interestingly, highly significant correlations were also noted between HCl-Fe and HCl-P as well as between HCl-Mn and HCl-Ca, and HCl-Fe and HCl-Al, thus suggesting that Fe, Mn and Al from clays were extracted alongside acid-soluble phases (apatite and carbonates). On the other hand, there is no correlation between NaOH-SRP and Al associated with this P binding pool at stations B and HB, while there is only a weak to moderate correlation at station N.

Table S4. Correlation between P and mobilized metals in P binding pools at station B. Highlighted values are significant at 0.05 level.

	BD-P	NaOH-SRP	HCl-P	HCl-Ca	Al-NaOH-SRP	HCl-Al	Si-NaOH-SRP	HCl-Si	BD-Mn	Mn-NaOH-SRP	HCl-Mn	BD-Fe	Fe-NaOH-SRP	HCl-Fe
BD-P	1.00													
NaOH-SRP	0.17	1.00												
HCl-P	-0.04	-0.22	1.00											
HCl-Ca	-0.13	-0.21	**0.42**	1.00										
Al-NaOH-SRP	**-0.40**	0.02	0.21	0.03	1.00									
HCl-Al	-0.01	-0.24	**0.36**	0.23	0.07	1.00								
Si-NaOH-SRP	0.03	-0.07	0.22	0.20	-0.13	**0.71**	1.00							
HCl-Si	0.03	-0.19	**0.49**	**0.45**	0.06	**0.72**	**0.65**	1.00						
BD-Mn	**0.47**	-0.09	-0.04	0.08	**-0.51**	-0.11	0.05	0.17	1.00					
Mn-NaOH-SRP	-0.17	-0.17	0.20	0.00	0.24	0.18	-0.03	-0.06	-0.25	1.00				
HCl-Mn	0.16	0.00	**0.46**	**0.39**	-0.11	**0.34**	0.22	**0.48**	**0.42**	0.30	1.00			
BD-Fe	**0.70**	-0.15	0.10	0.07	**-0.36**	0.15	0.26	**0.31**	**0.56**	**0.38**	**0.35**	1.00		
Fe-NaOH-SRP	0.17	0.21	0.09	0.10	-0.14	0.04	0.23	0.18	**0.39**	-0.13	**0.36**	0.12	1.00	
HCl-Fe	0.01	-0.21	**0.63**	**0.38**	0.06	**0.79**	**0.61**	**0.72**	0.02	0.20	**0.59**	**0.32**	0.09	1.00

Table S5. Correlation between P and mobilized metals in P binding pools at station N. Highlighted values are significant at 0.05 level.

	BD-P	***NaOH-SRP***	***HCl-P***	***HCl-Ca***	***Al-NaOH-SRP***	***HCl-Al***	***Si-NaOH-SRP***	***HCl-Si***	***BD-Mn***	***Mn-NaOH-SRP***	***HCl-Mn***	***BD-Fe***	***Fe-NaOH-SRP***	***HCl-Fe***
BD-P	1.00													
NaOH-SRP	**0.37**	1.00												
HCl-P	**-0.33**	0.02	1.00											
HCl-Ca	-0.16	0.12	**0.56**	1.00										
Al-NaOH-SRP	0.00	**0.46**	0.22	**0.31**	1.00									
HCl-Al	-0.15	0.01	**0.80**	**0.65**	**0.35**	1.00								
Si-NaOH-SRP	-0.01	**0.34**	0.29	0.30	**0.85**	**0.40**	1.00							
HCl-Si	-0.04	**0.31**	0.08	**0.67**	**0.43**	0.13	**0.41**	1.00						
BD-Mn	**0.82**	**0.32**	**-0.37**	-0.08	0.13	-0.19	0.04	0.12	1.00					
Mn-NaOH-SRP	-0.08	-0.06	**0.54**	**0.51**	**0.37**	**0.64**	**0.37**	0.21	-0.11	1.00				
HCl-Mn	0.26	**0.43**	**0.50**	**0.47**	0.01	**0.49**	0.13	0.11	0.18	0.19	1.00			
BD-Fe	**0.82**	**0.38**	**-0.33**	-0.10	0.10	-0.02	0.08	-0.05	**0.77**	0.00	**0.34**	1.00		
Fe-NaOH-SRP	0.10	**0.50**	-0.15	0.29	**0.52**	-0.06	**0.33**	**0.60**	0.16	0.02	0.14	0.14	1.00	
HCl-Fe	-0.16	0.09	**0.80**	**0.67**	**0.32**	**0.89**	**0.38**	0.15	-0.19	**0.49**	**0.65**	-0.04	-0.09	1

Table S6. Correlation between P and mobilized metals in P binding pools at station HB. Highlighted values are significant at 0.05 level.

	BD-P	***NaOH-SRP***	***HCl-P***	***HCl-Ca***	***Al-NaOH-SRP***	***HCl-Al***	***Si-NaOH-SRP***	***HCl-Si***	***BD-Mn***	***Mn-NaOH-SRP***	***HCl-Mn***	***BD-Fe***	***Fe-NaOH-SRP***	***HCl-Fe***
BD-P	1													
NaOH-SRP	**0.66**	1												
HCl-P	-0.01	0.34	1											
HCl-Ca	0.03	-0.21	**0.46**	1										
Al-NaOH-SRP	0.21	0.21	0.15	0.16	1									
HCl-Al	-0.03	**-0.41**	0.01	**0.78**	0.30	1								
Si-NaOH-SRP	-0.19	-0.25	-0.06	0.33	**-0.47**	0.36	1							
HCl-Si	0.08	-0.14	0.11	**0.60**	**0.63**	**0.71**	0.08	1						
BD-Mn	**0.93**	**0.72**	0.10	0.11	0.28	0.05	-0.25	0.12	1					
Mn-NaOH-SRP	**0.70**	**0.77**	0.05	-0.10	**0.38**	-0.08	-0.37	-0.01	**0.81**	1				
HCl-Mn	0.34	**0.61**	**0.83**	0.24	0.06	-0.28	-0.22	-0.08	**0.43**	0.28	1			
BD-Fe	**0.87**	**0.76**	0.05	-0.09	0.23	-0.20	-0.37	0.07	**0.89**	**0.72**	**0.45**	1		
Fe-NaOH-SRP	0.21	**0.44**	0.20	-0.07	0.31	-0.22	**-0.38**	0.04	0.22	**0.54**	0.32	0.26	1	
HCl-Fe	0.05	-0.25	0.12	**0.77**	**0.52**	**0.92**	0.19	**0.88**	0.14	-0.02	-0.13	-0.01	-0.11	1

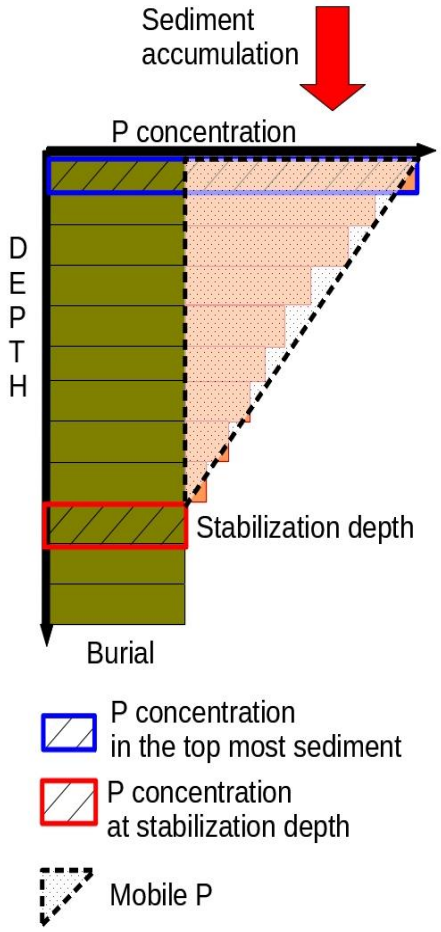

Figure S1 Schematic presentation of relationships between P burial, accumulation, stabilization depth and mobile P

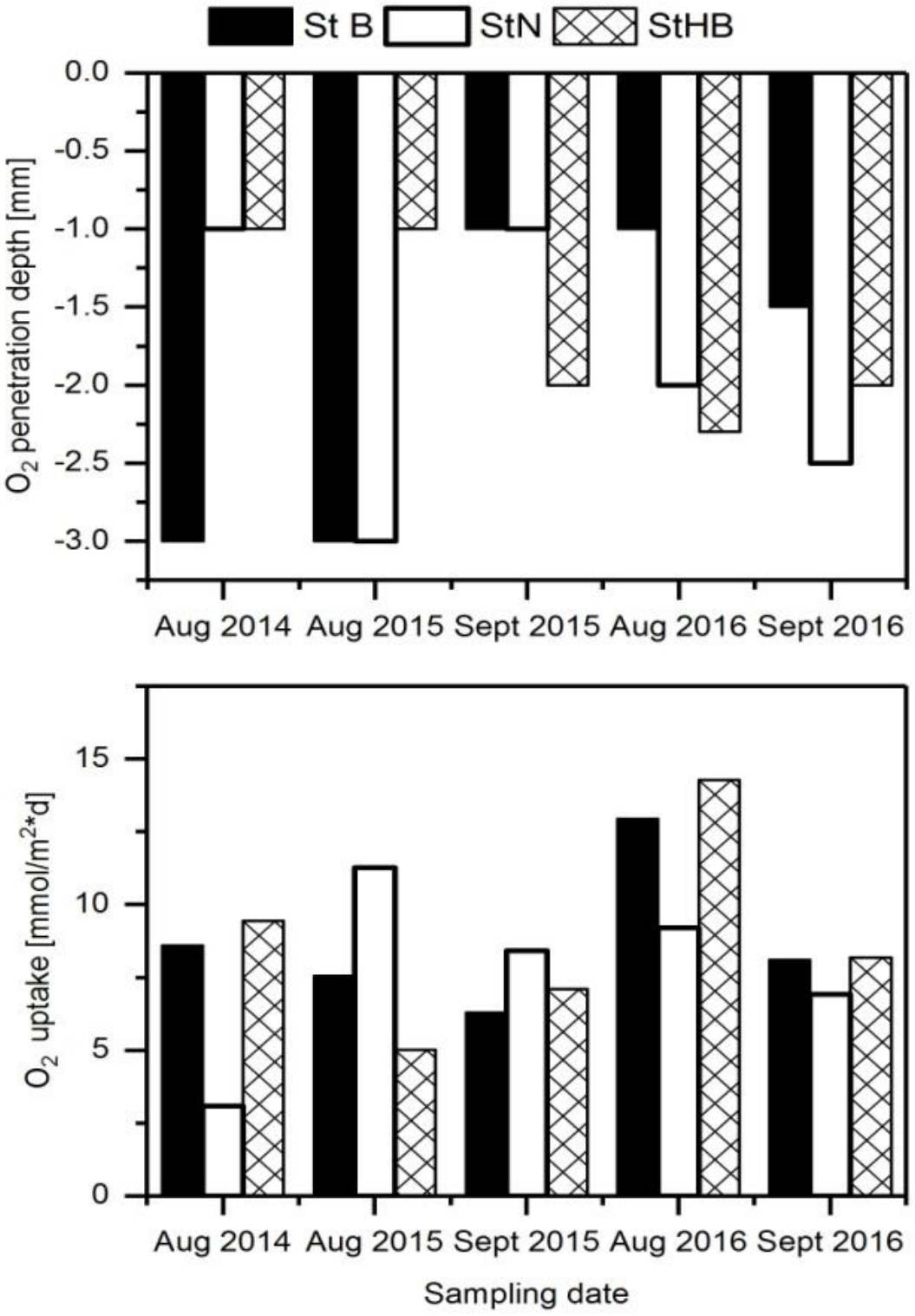

Figure S2 Oxygen penetration (top panel) and uptake (lower panel).

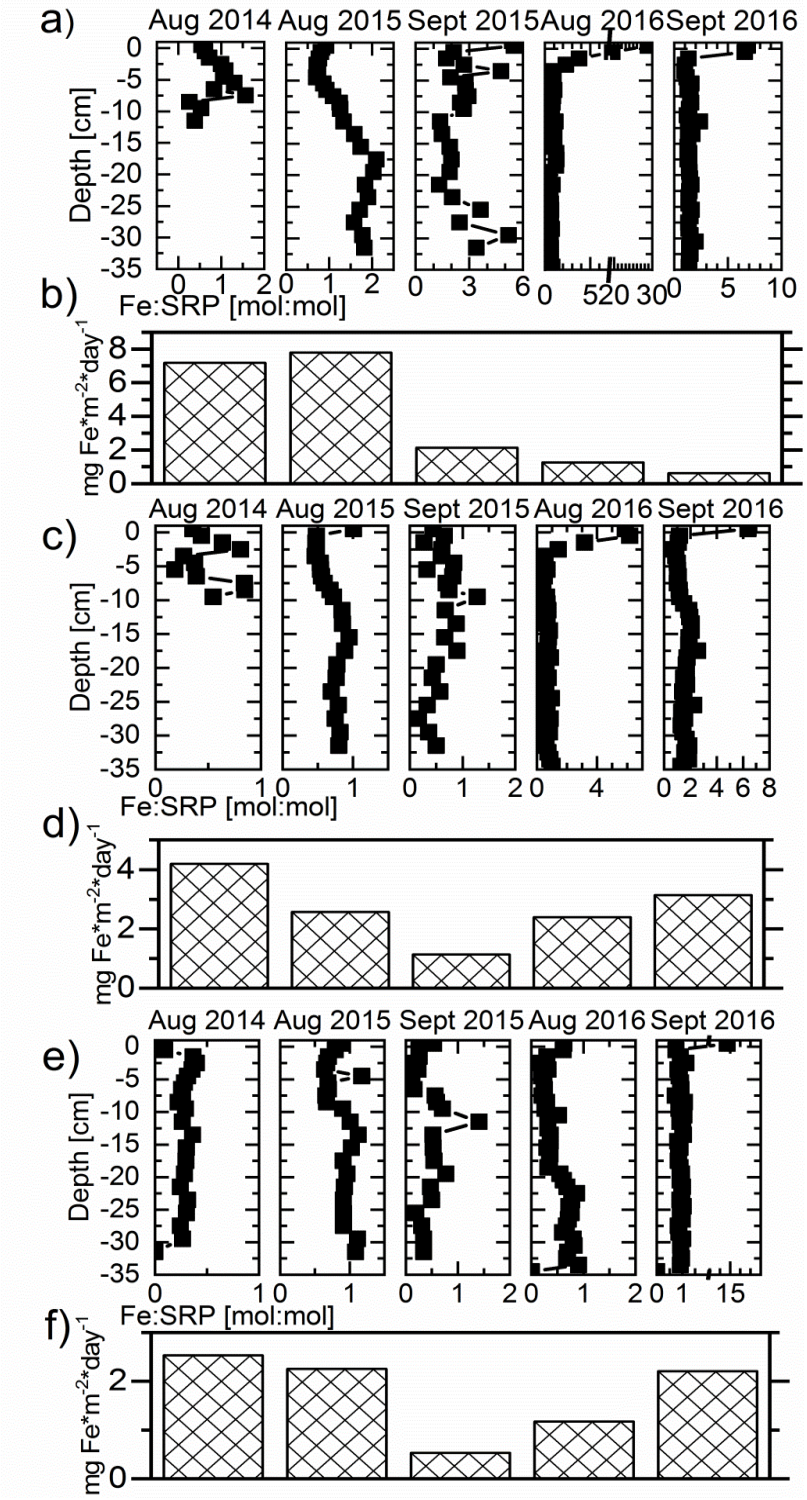

Figure S3. Fe:SRP molar ratios in pore water: (a) station B, (c) station N and (e) station HB. Diffusive Fe fluxes from sediments: (b) station B, (d) station N and (f) station HB.

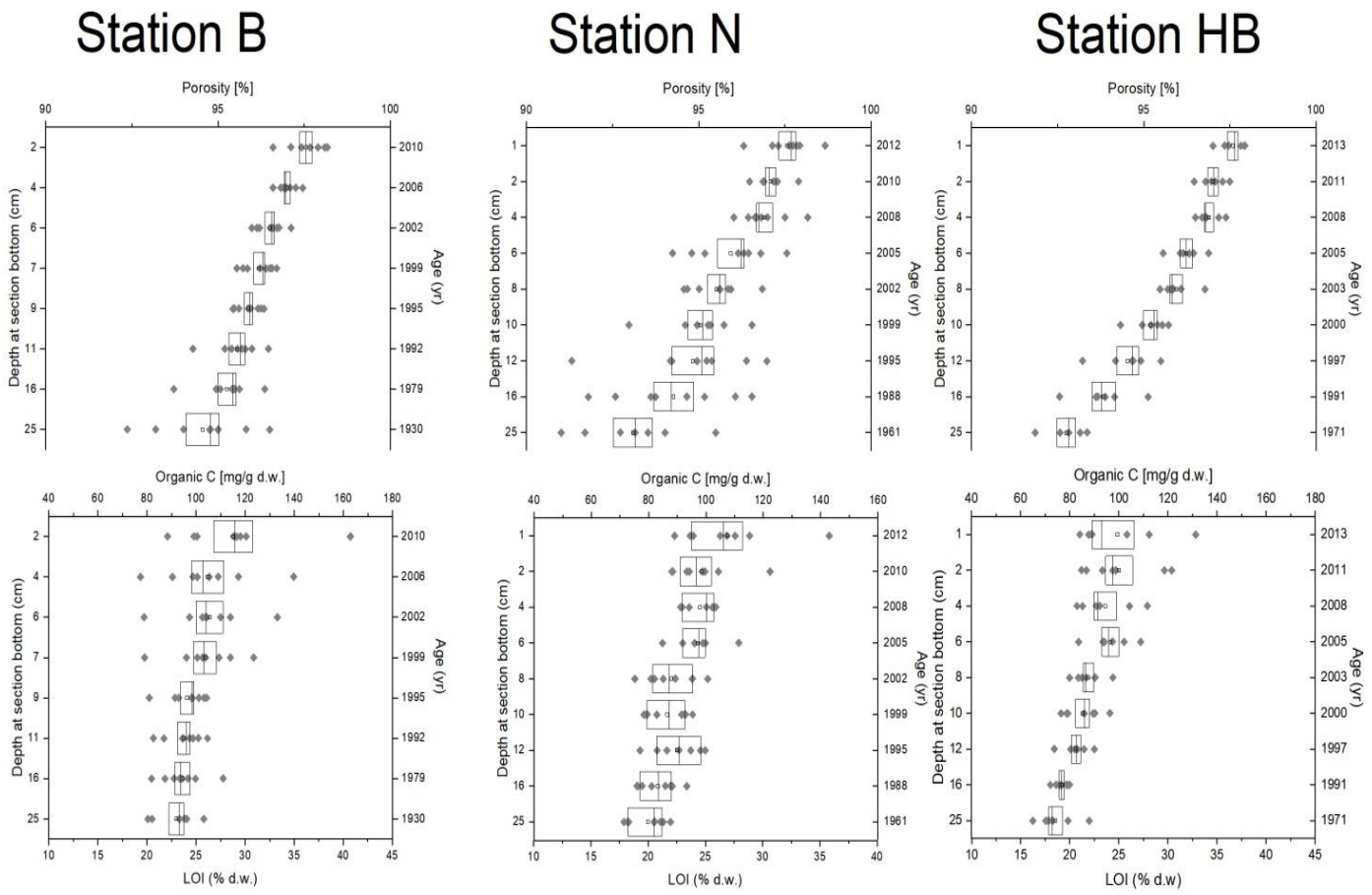

Figure S4: Porosity, loss on ignition and organic matter in Bay of Quinte sediments (2013-2016 sampling dates); LOI is converted to organic carbon assuming organic matter composition as CH_2O

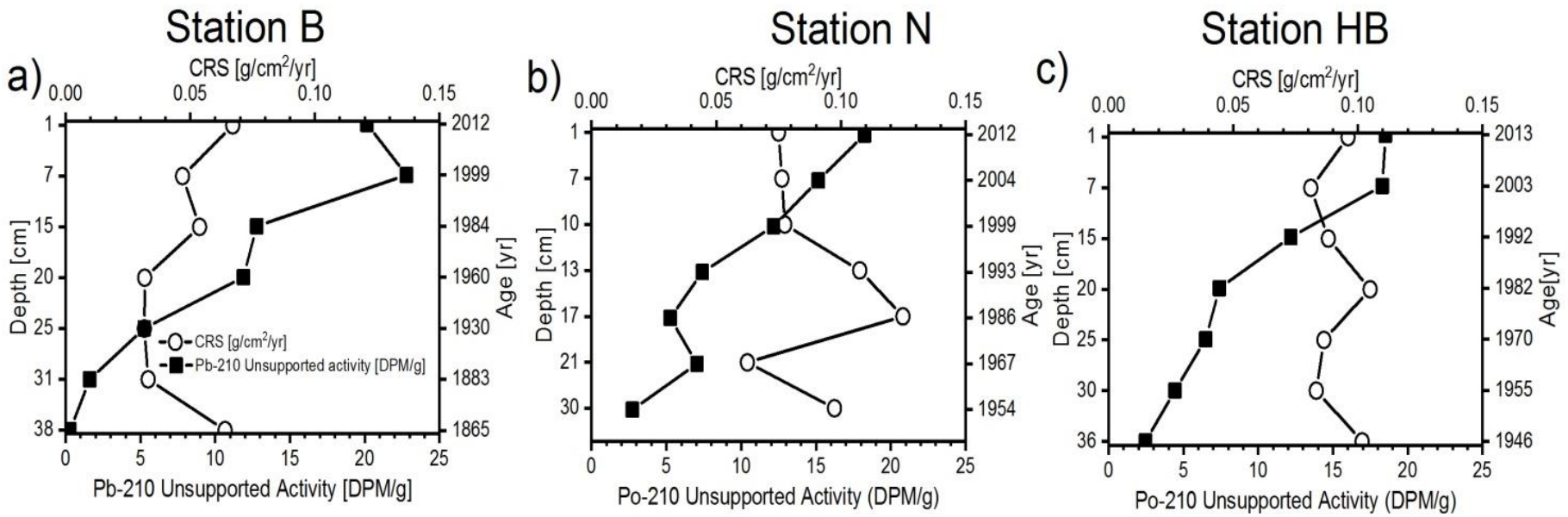

Figure S5: Pb core dating and sedimentation rates

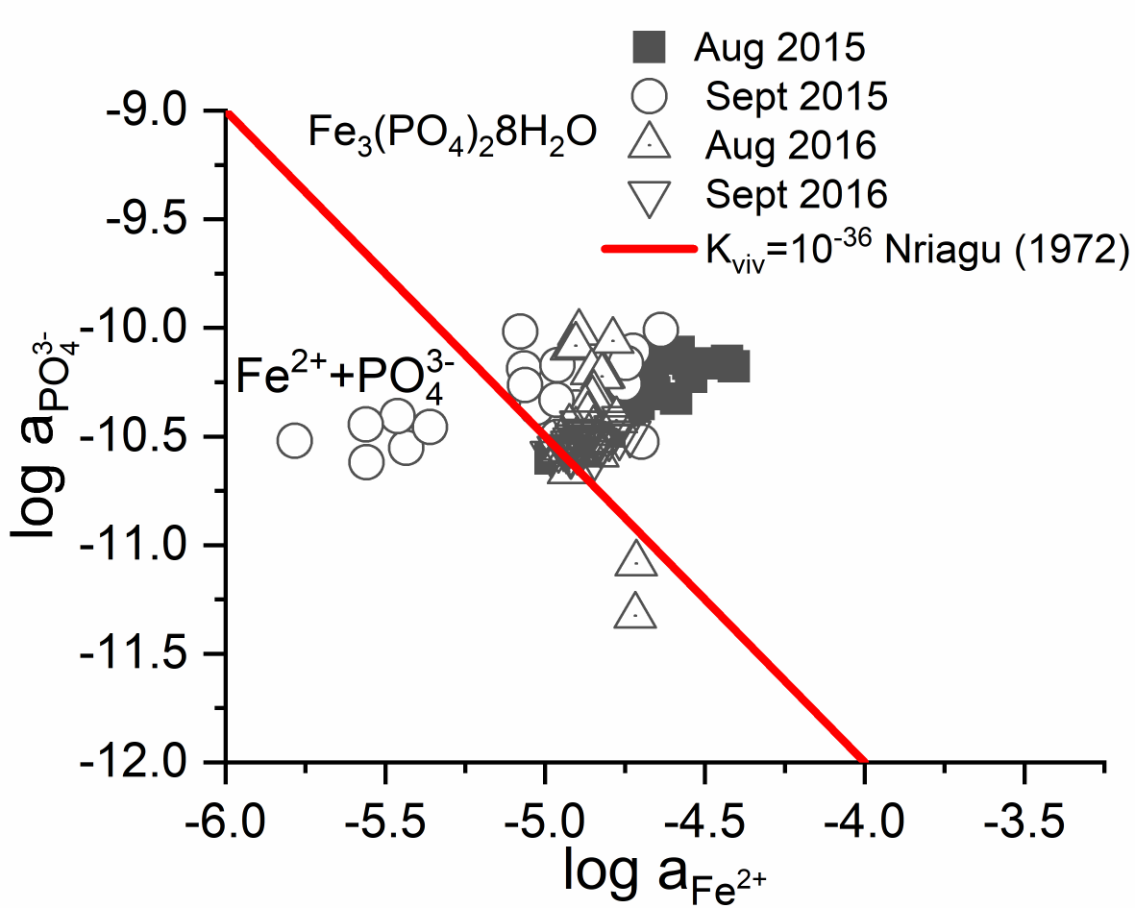

Figure S6. Ion activities of phosphate and iron in the porewater at station HB, calculated using PHREEQC (Parkhurst and Appelo 2013. The diagonal red line in the diagram represents the vivianite solubility constant Kviv = 1×10^{-36} given by Nriagu (1972).

References

Jeroschewski, P. 1996. An amperometric microsensor for the determination off H2S in aquatic environments. Anal. Chem. **68**: 4351–4357. doi:10.1021/ac960091b

Maerki, M., B. Müller, C. Dinkel, and B. Wehrli. 2009. Mineralization pathways in lake sediments with different oxygen and organic carbon supply. Limnol. Oceanogr. **54**: 428–438. doi:10.4319/lo.2009.54.2.0428

Manning P.G., 1996. Bioavailability of riverine, sewage plant, and sediment phosphorus in the Bay of Quinte, Lake Ontario, Can. Mineral. **34**, 667–675.

Nriagu, J.O., 1972. Stability of vivianite and ion-pair formation in the system Fe3(PO4)2-$H_3PO_4$$H_3PO_4$-$H_2O$. Geochim. Cosmochim. Acta **36**, 459–470. https://doi.org/10.1016/0016-7037(72)90035-X

Parkhurst, D.L., Appelo, C.A.J., 2013. PHREEQC (Version 3)-A Computer Program for Speciation, Batch-Reaction, One-Dimensional Transport, and Inverse Geochemical Calculations. Model. Tech. B. 6 497. https://doi.org/Rep. 99-4259